A decorative graphic on a blue background. It features a large orange circle on the left, a smaller white circle above it, a green circle below it, and a large blue circle on the right. A white rounded rectangle is centered in the middle, containing red text. The text is arranged in four lines, centered within the white box.

**Detecting ultra-light
particles from
astrophysical observations
and quantum sensors**

Outline

- Introduction
- Probing DPDM from Gaia (Position/velocity)
- Probing DPDM from PTA (Time)
- EHT polarimetric measurements on axion cloud from SMBH
- Detecting axion through the Superconducting Radio Frequency Cavity.
- Summary

High energy physics

TeV

GeV

MeV

eV

t

W, Z h 2012

τ b
 μ c
u, d s

p, n

nucleus

12 orders of magnitude

e

ν_3

ν_2

ν_1

atoms

1895

Open the door of sub-atom physics

Higher and higher energy

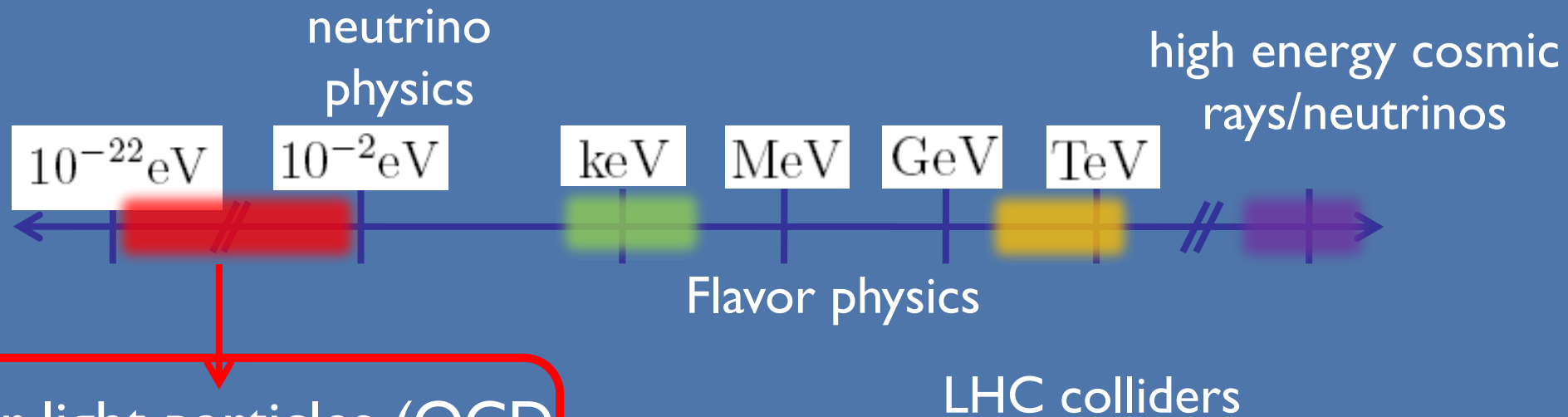
Last 122 years

Extremely successful!



Not just higher energy

Besides the higher and higher energies, we may consider other extreme environment to search for NP



Super light particles (QCD, axion, ALPs, DP,)

Table top exp: Cavity, LC circuit, quantum sensor, etc.

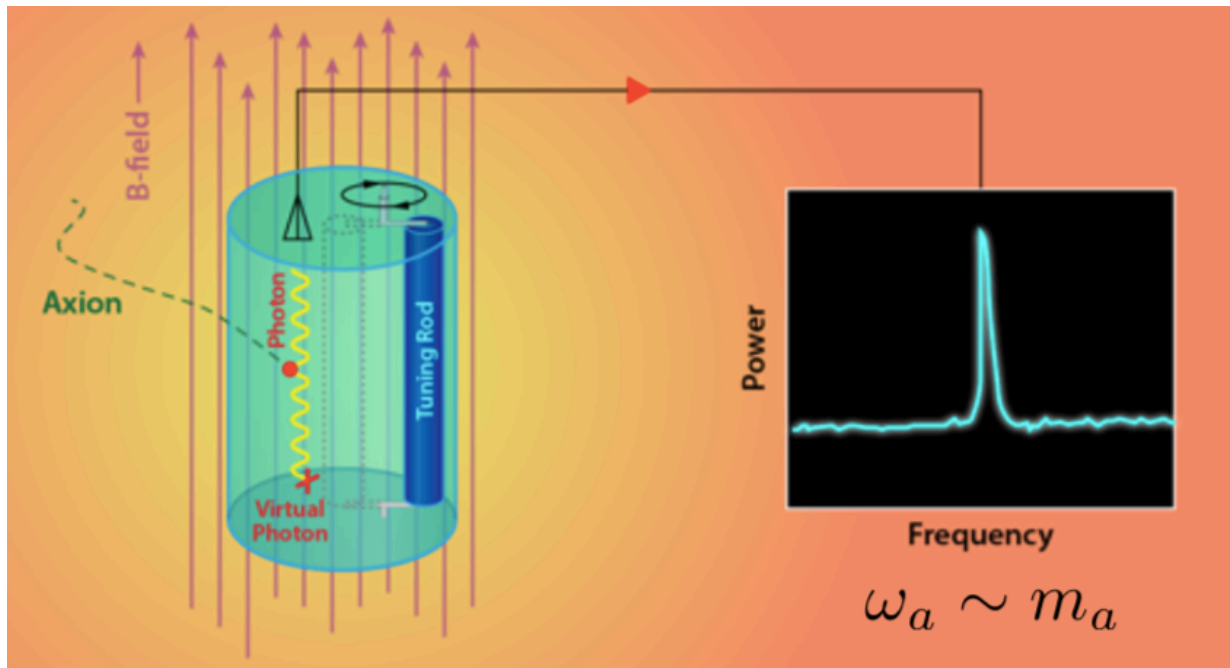
Astrophysical exp: Radio signal, sun, GWs, supernova, etc.

Cavity with static B field

$$\left(\partial_t^2 + \frac{m_a}{Q_1} \partial_t + m_a^2 \right) \mathbf{E}_1 \sim m_a \cos m_a t$$

$$Q_a \sim 10^6$$

$$m_a \sim \text{GHz} \sim 10^{-6} \text{ eV}$$

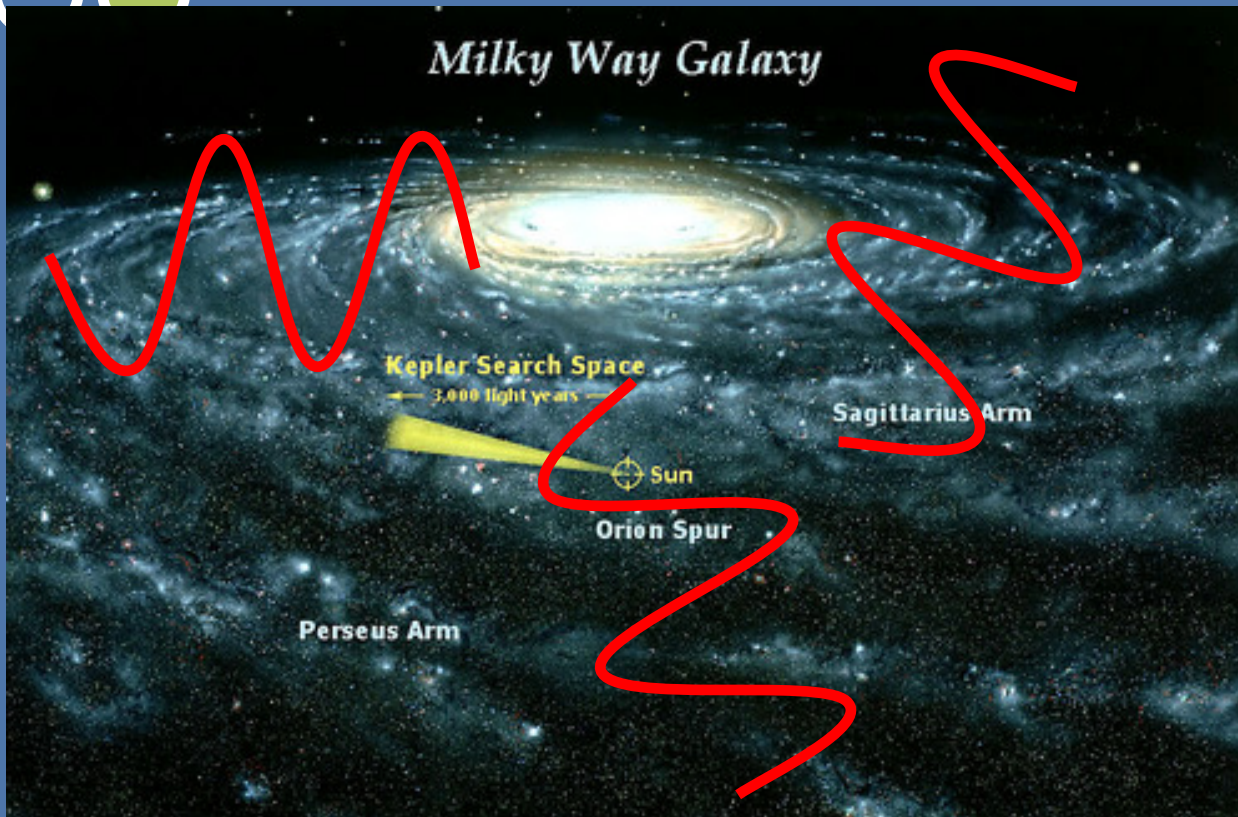


Compton wavelength

Cavity size \sim (axion mass)⁻¹

e.g. ADMX, HAYSTACK

Ultra-light DM



Difficult to detect, need astrophysical observations.

De Broglie wavelength
~ the soliton core

For ultra-light DM ($\sim 10^{-22}$ eV), they form super low frequency (nHz) oscillating backgrounds

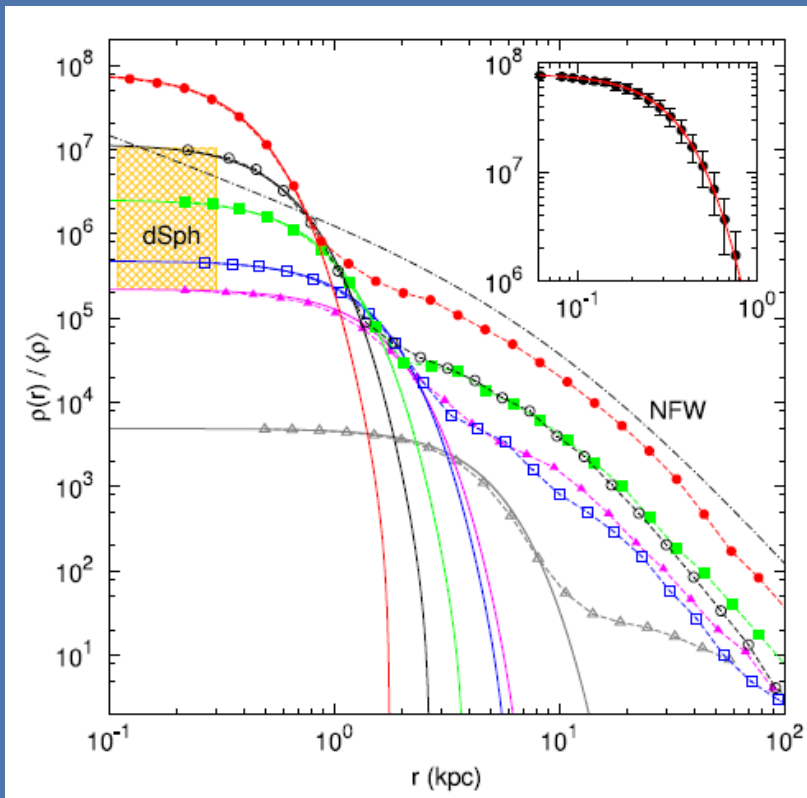
A decorative graphic on a blue background. It features a large orange circle on the left, a smaller white circle above it, a green circle below it, and a large blue circle on the right. A white rounded rectangle is centered in the middle, containing the title text. The circles are connected by thin white lines.

Probing DPDM through Gaia

H-k. Guo, Y-q. Ma, [J. Shu.](#), X. Xiao, Q. Yuan, Y. Zhao,
arxiv: 1902.05962 JCAP 1905 (2019) 015

Fussy DM

Excellent ultralight DM candidate



Ultra-light bosonic DM can cause BEC, and behave like CDM at large scale

At small scale (comparing to wavelength, $m \sim 10^{-22}$ eV, $\lambda \sim$ kpc), it can be used to solve the cusp-core problem

Hu et al., 2000

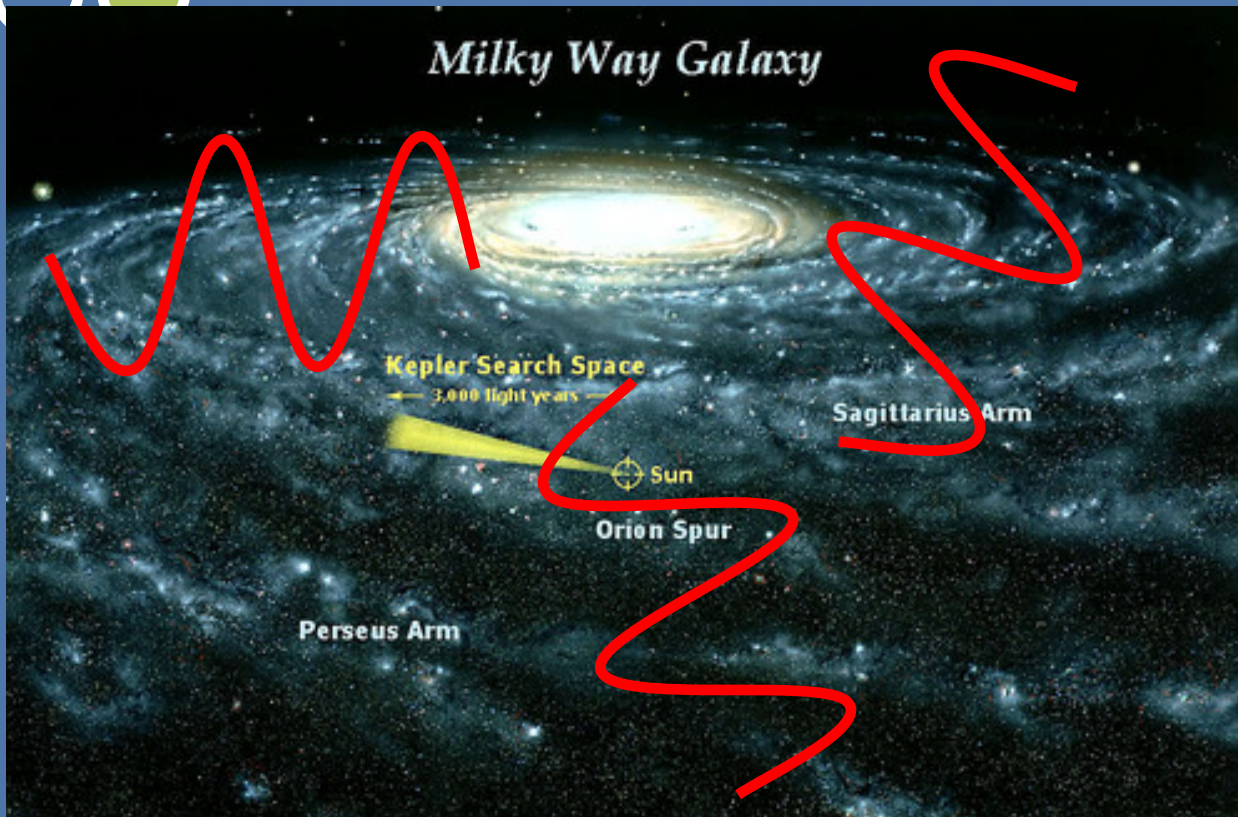
Ultralight DM is expected to have a soliton core

$$\rho(x) = \begin{cases} 0.019 \left(\frac{m_a}{m_{a,0}} \right)^{-2} \left(\frac{l_c}{1 \text{ kpc}} \right)^{-4} M_{\odot} \text{pc}^{-3}, & \text{for } r < l_c \\ \frac{\rho_0}{r/R_H (1+r/R_H)^2}, & \text{for } r > l_c \end{cases}$$

soliton solution

NFW profile

Ultra-light DM



Difficult to detect, need astrophysical observations.

For ultra-light DM ($\sim 10^{-22}$ eV), they form super low frequency (nHz) oscillating backgrounds

Ultra-light DPDM

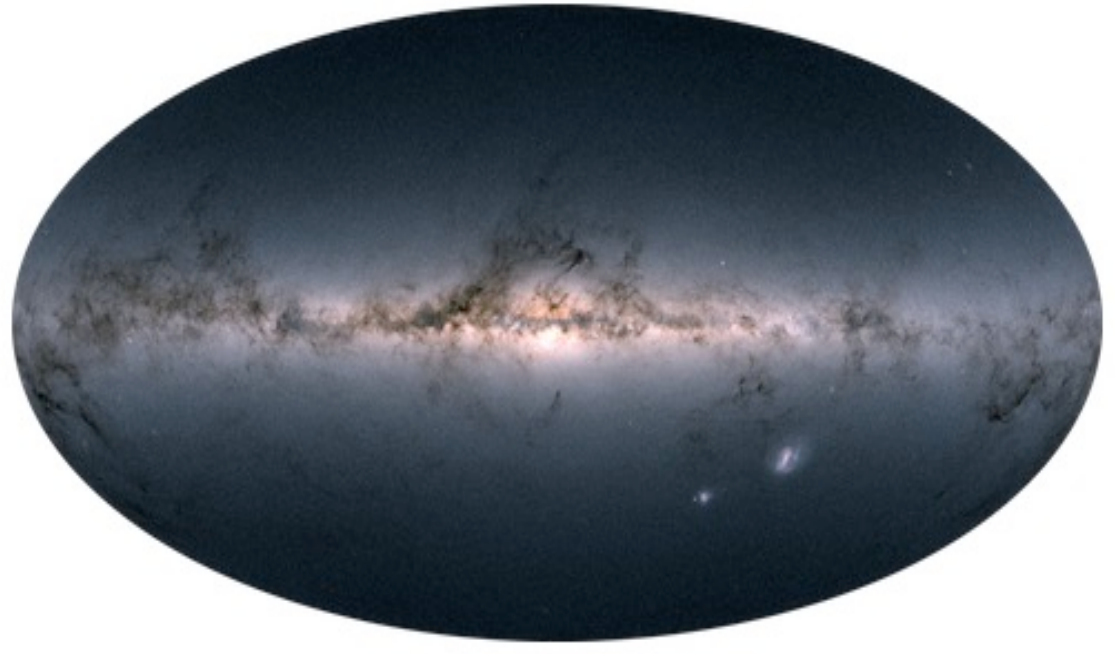
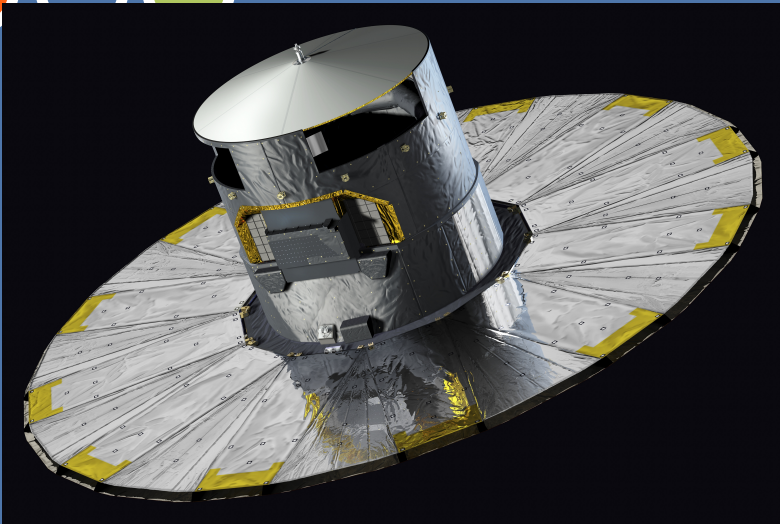
A hypothetical hidden-sector particle proposed as a force carrier similar to photon

Considering a special class of dark photon which is the gauge boson of the $U(1)_B$ or $U(1)_{B-L}$ group: it would interact with any object with B or (B-L) number (“dark charge”)

A good candidate of (fuzzy) dark matter (DPDM)

If its is very small (10^{-22} eV), the dark photon behaves like an oscillating background, drives displacements for particles with “dark charge”

Precision of star position



Gaia satellite (2013), plan to accurately measure 1% of star inside the Milky Way ($\sim 10^9$) for their position and speed.

Expect breakthrough in the Milky Way structure, evolution of stars, new planet, fundamental physics, etc.

Aberration of Light

Objects (Gaia satellite) feel an oscillating acceleration in the DPDM backgrounds

$$\mathbf{a}(t, \mathbf{x}) \simeq \epsilon e \frac{q}{m} m_A \mathbf{A}_0 \cos(m_A t - \mathbf{k} \cdot \mathbf{x})$$

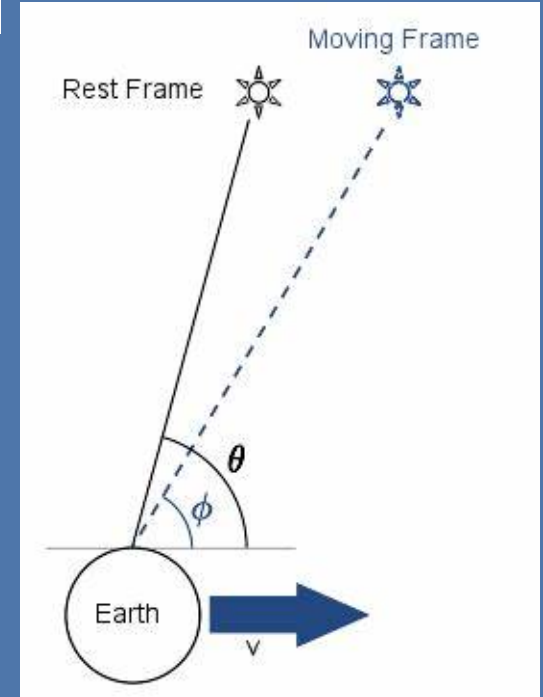
This acceleration will cause the velocity to have a periodic change, therefore periodically shift the position of the star from the observer

$$\Delta \mathbf{v}(t, \mathbf{x}) \simeq \epsilon e \frac{q}{m} \mathbf{A}_0 \sin(m_A t - \mathbf{k} \cdot \mathbf{x}).$$

$$\Delta \theta \simeq -\Delta v \sin \theta$$

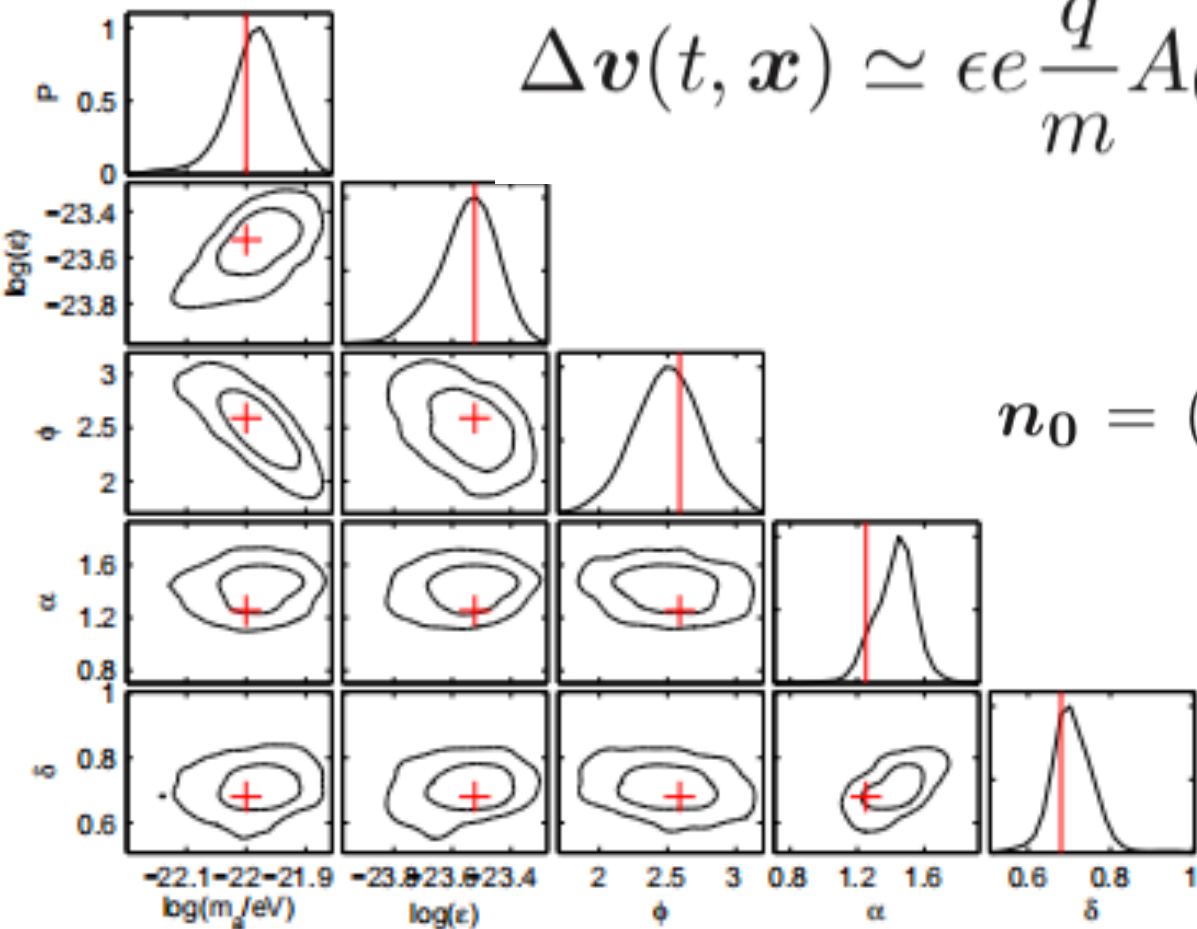
radial direction not very accurate

A large sample of the star position period variation will hint the signal.



Gaia search for ultra-light DPDM

$$\Delta \mathbf{v}(t, \mathbf{x}) \simeq \epsilon e \frac{q}{m} A_0 \mathbf{n}_0 \sin[m_A(t - t_0) + \phi],$$



equatorial coordinate (α, δ)

$$\mathbf{n}_0 = (\cos \delta \cos \alpha, \cos \delta \sin \alpha, \sin \delta),$$

Compressed data,
high accretion

$$\sigma = 100 \mu\text{as}/\sqrt{10^5}.$$

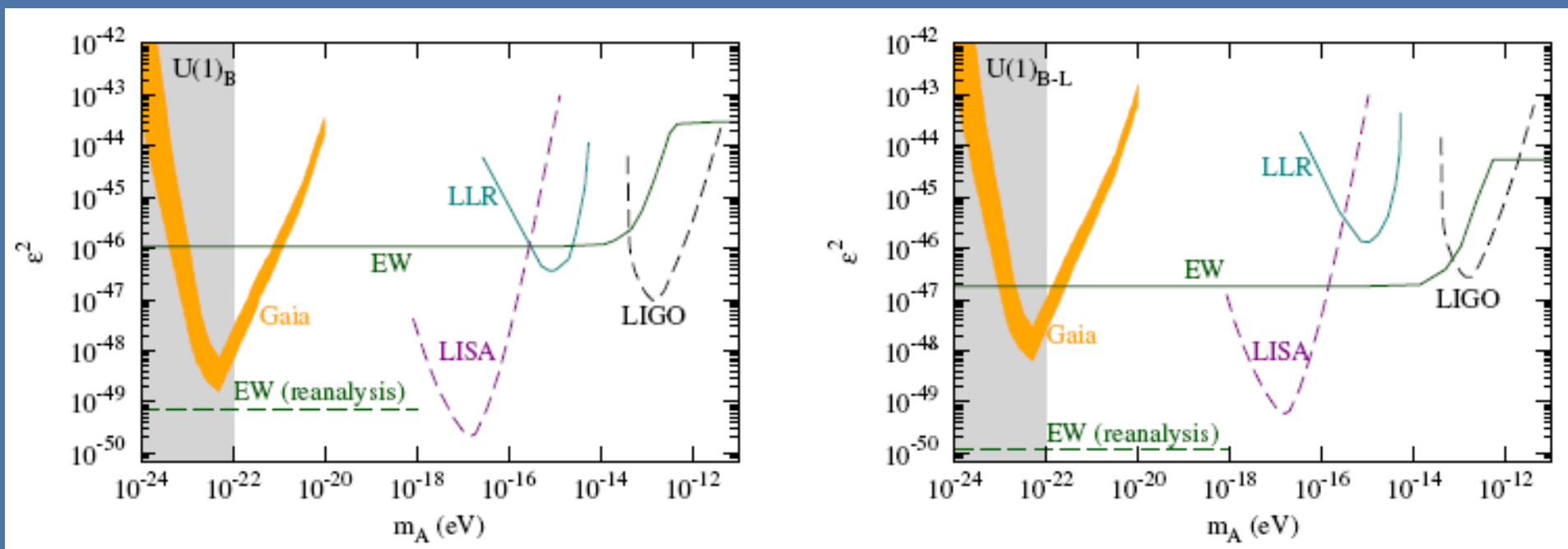
mock data

H-k. Guo, Y-q. Ma, [J. Shu.](#), X. Xiao, Q. Yuan, Y. Zhao, JCAP 1905 (2019) 015

$$(m_A, \epsilon, \phi, \alpha, \delta) = (10^{-22} \text{ eV}, 3 \times 10^{-24}, 2.59, 1.25, 0.68).$$

Gaia search for ultra-light DPDM

95% C.L. exclusion by varying mass and coupling constant



H-k. Guo, Y-q. Ma, [J. Shu.](#), X. Xiao, Q. Yuan, Y. Zhao, JCAP 1905 (2019) 015

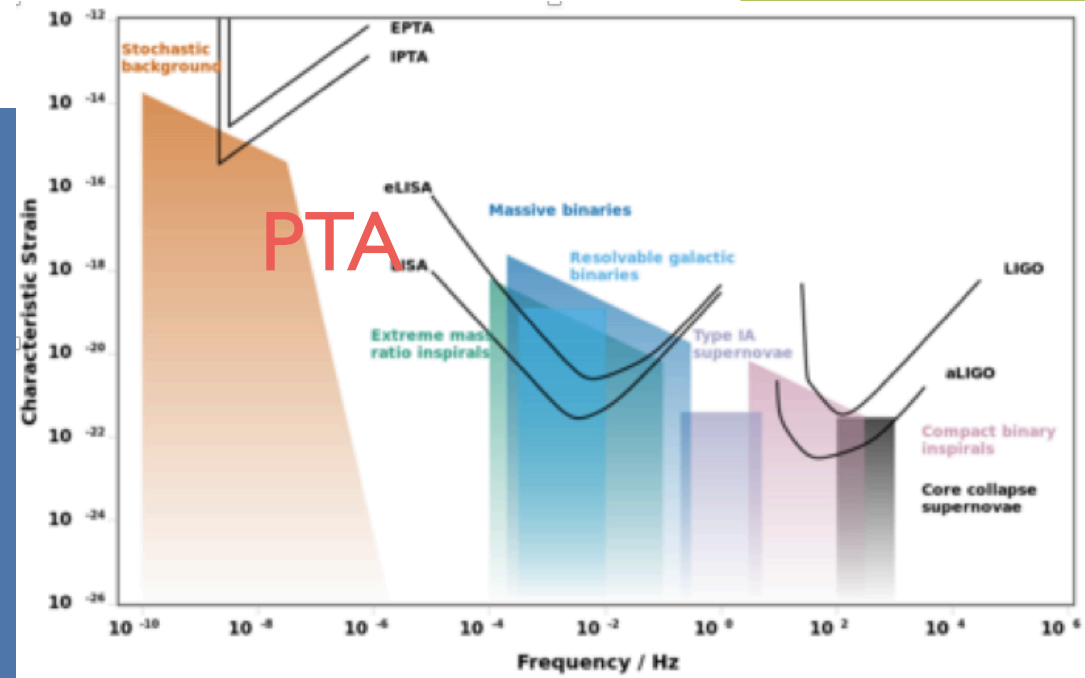
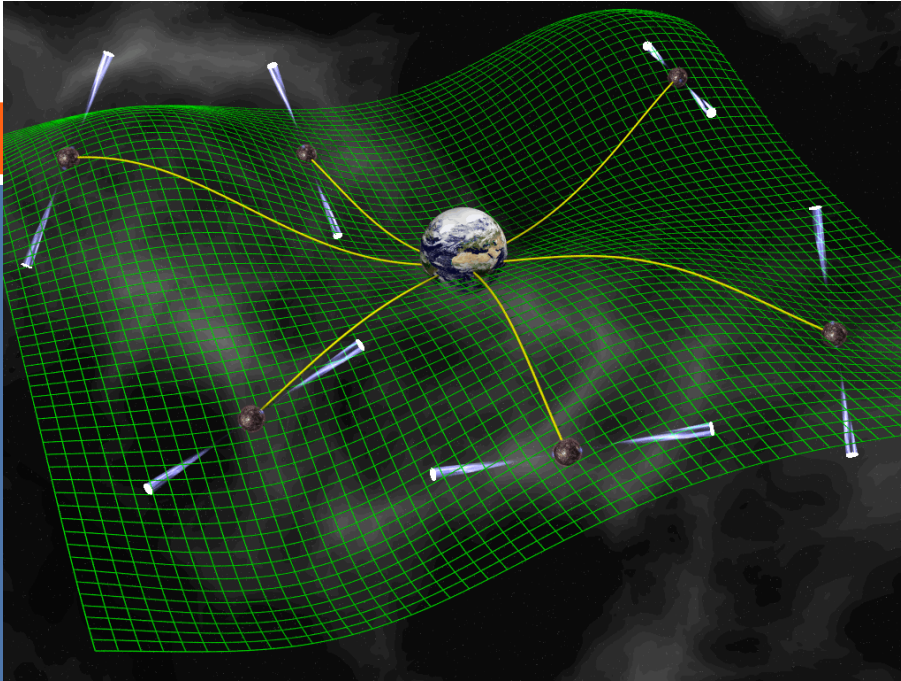
Future Gaia final data release will give you the real data **with time sequence**

A decorative graphic on a blue background. It features a large white rounded rectangle in the center. To the left of this rectangle is a large orange circle, and below it is a smaller green circle. To the right of the rectangle is a green circle above a larger blue circle. A white outline of a circle is positioned above the white rectangle. All shapes are connected by thin white lines.

Probing DPDM through PTA

J. Shu., X. Xiao, Z-j. Xia, Q. Yuan, Y. Zhao, X-j. Zhu, with PPTA collaboration, in preparation

The pulsar timing array (PTA)



mili-seconds pulsar is the stablest “clock” in cosmology.

accurately measure the change of the time pulse can
be used to probe nHz gravitational waves

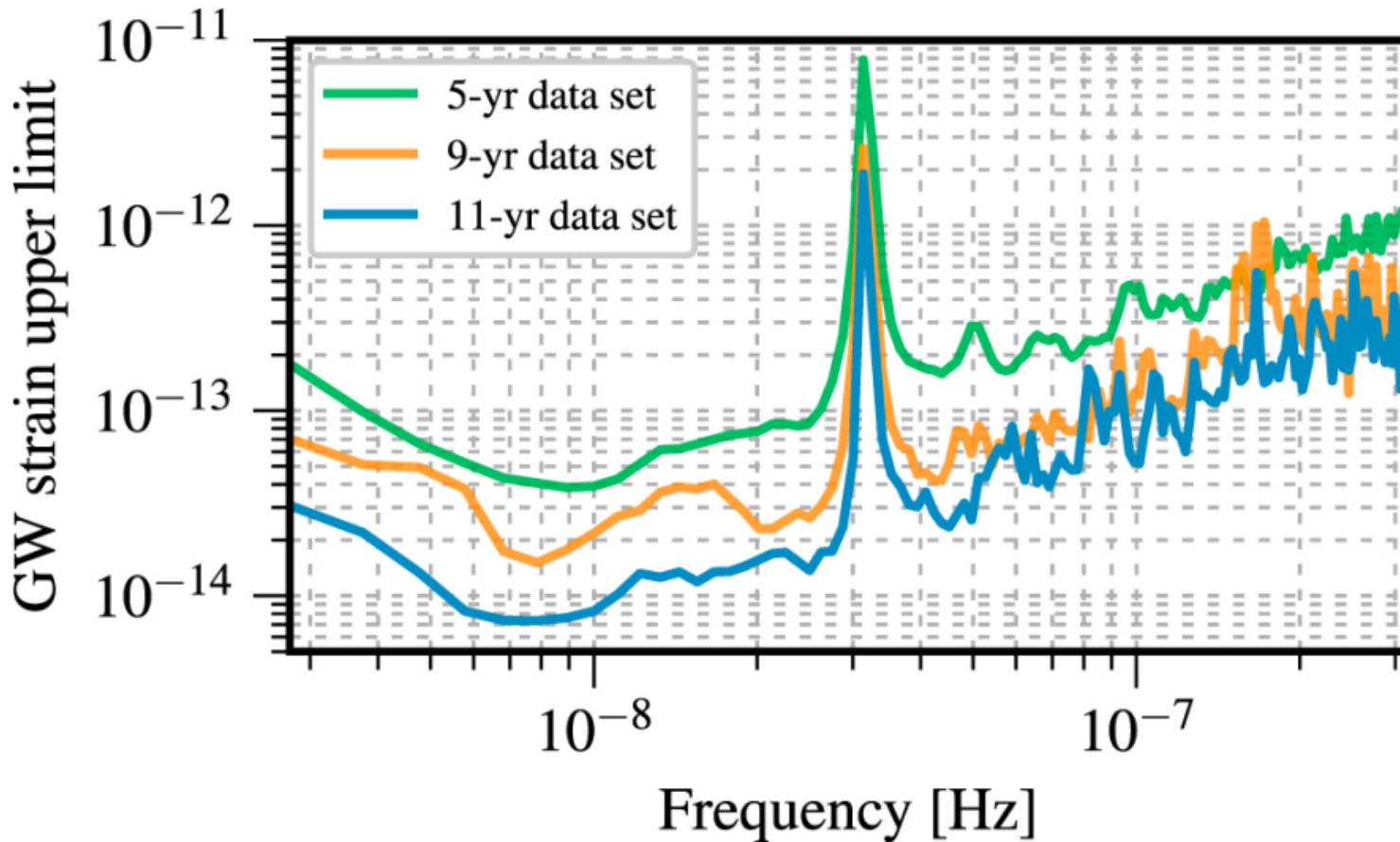
Can be used to probe other fundamental physics like DM

PPTA, EPTA, IPTA, NanoGrav, **CPTA**(FAST)?

未来平方公里阵列(SKA)



Sensitivity of GW search from NANOGrav PTA



Aggarwal et al. (2019)

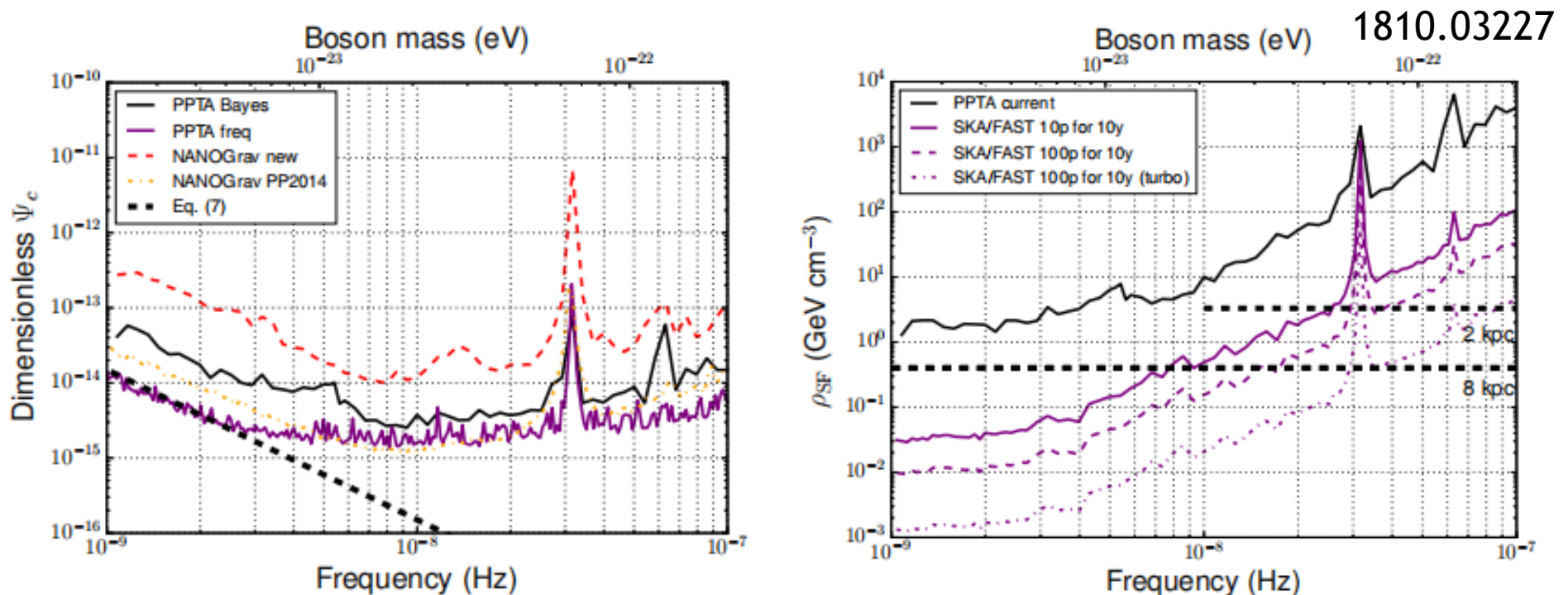
“Anomalies” for power law SGWB recently

can be interpreted from the PBH, cosmic defects, phase transition
will be checked by other collaborations, like PPTA next year.

PPTA search for scalar fuzzy DM

Parkes Pulsar Timing Array constraints on ultralight scalar-field dark matter

Nataliya K. Porayko,^{1,*} Xingjiang Zhu,^{2,3,4,†} Yuri Levin,^{5,6,2} Lam Hui,⁵ George Hobbs,⁷ Aleksandra Grudskaya,⁸ Konstantin Postnov,^{8,9} Matthew Bailes,^{10,4} N. D. Ramesh Bhat,¹¹ William Coles,¹² Shi Dai,⁷ James Dempsey,¹³ Michael J. Keith,¹⁴ Matthew Kerr,¹⁵ Michael Kramer,^{1,14} Paul D. Lasky,^{2,4} Richard N. Manchester,⁷ Stefan Osłowski,¹⁰ Aditya Parthasarathy,¹⁰ Vikram Ravi,¹⁶ Daniel J. Reardon,^{10,4} Pablo A. Rosado,¹⁰ Christopher J. Russell,¹⁷ Ryan M. Shannon,^{10,4} Renée Spiewak,¹⁰ Willem van Straten,¹⁸ Lawrence Toomey,⁷ Jingbo Wang,¹⁹ Linqing Wen,^{3,4} and Xiaopeng You²⁰
(The PPTA Collaboration)



Future SKA can have much better results!

Parkes PTA数据



64m Parkes telescope in Australia

Pulsars	N_{obs}	T(years)	$\bar{\sigma} \times 10^{-6}(s)$	$\log_{10} A_{SN}$	γ_{SN}	$\log_{10} A_{DM}$	γ_{DM}
J0437-4715	29262	15.03	0.296	$-15.76^{+0.17}_{-0.18}$	$6.63^{+0.17}_{-0.13}$	$-13.05^{+0.10}_{-0.08}$	$2.26^{+0.32}_{-0.44}$
J0613-0200	5920	14.20	2.504	$-14.63^{+0.77}_{-0.68}$	$4.93^{+1.33}_{-1.61}$	$-13.02^{+0.08}_{-0.08}$	$0.95^{+0.33}_{-0.31}$
J0711-6830	5547	14.21	6.197	$-12.85^{+0.14}_{-0.16}$	$0.97^{+0.64}_{-0.55}$	$-14.54^{+0.72}_{-0.89}$	$4.43^{+1.68}_{-1.72}$
J1017-7156	4053	7.77	1.577	$-12.89^{+0.07}_{-0.07}$	$0.54^{+0.53}_{-0.37}$	$-12.72^{+0.06}_{-0.06}$	$2.18^{+0.45}_{-0.44}$
J1022+1001	7656	14.20	5.514	$-12.79^{+0.12}_{-0.13}$	$0.54^{+0.55}_{-0.37}$	$-13.04^{+0.10}_{-0.12}$	$0.58^{+0.47}_{-0.36}$
J1024-0719	2643	14.09	4.361	$-14.28^{+0.27}_{-0.20}$	$6.51^{+0.35}_{-0.60}$	$-14.53^{+0.54}_{-0.56}$	$5.22^{+1.14}_{-1.18}$
J1045-4509	5611	14.15	9.186	$-12.75^{+0.24}_{-0.40}$	$1.58^{+1.28}_{-0.93}$	$-12.18^{+0.09}_{-0.08}$	$1.86^{+0.36}_{-0.32}$
J1125-6014	1407	12.34	1.981	$-12.64^{+0.11}_{-0.12}$	$0.51^{+0.55}_{-0.37}$	$-13.14^{+0.19}_{-0.21}$	$3.36^{+0.73}_{-0.66}$
J1446-4701	508	7.36	2.200	$-16.46^{+2.88}_{-3.17}$	$2.74^{+2.49}_{-1.89}$	$-13.49^{+0.32}_{-1.87}$	$2.48^{+1.92}_{-1.45}$
J1545-4550	1634	6.97	2.249	$-17.33^{+2.50}_{-2.55}$	$3.25^{+2.45}_{-2.18}$	$-13.40^{+0.24}_{-0.38}$	$3.90^{+1.61}_{-1.09}$
J1600-3053	7047	14.21	2.216	$-17.63^{+2.10}_{-2.29}$	$3.28^{+2.34}_{-2.15}$	$-13.27^{+0.12}_{-0.13}$	$2.79^{+0.43}_{-0.40}$
J1603-7202	5347	14.21	4.947	$-12.82^{+0.14}_{-0.16}$	$1.01^{+0.67}_{-0.60}$	$-12.66^{+0.10}_{-0.09}$	$1.44^{+0.40}_{-0.38}$
J1643-1224	5941	14.21	4.039	$-12.32^{+0.08}_{-0.09}$	$0.51^{+0.42}_{-0.34}$	$-12.27^{+0.07}_{-0.07}$	$0.55^{+0.32}_{-0.29}$
J1713+0747	7804	14.21	1.601	$-14.09^{+0.25}_{-0.38}$	$2.98^{+1.00}_{-0.64}$	$-13.35^{+0.08}_{-0.08}$	$0.53^{+0.32}_{-0.31}$
J1730-2304	4549	14.21	5.657	$-17.39^{+2.39}_{-2.51}$	$3.05^{+2.59}_{-2.12}$	$-14.11^{+0.40}_{-0.57}$	$4.22^{+1.42}_{-1.04}$
J1732-5049	807	7.23	7.031	$-16.51^{+3.04}_{-2.97}$	$3.29^{+2.37}_{-2.97}$	$-13.38^{+0.54}_{-0.84}$	$4.07^{+1.96}_{-1.93}$
J1744-1134	6717	14.21	2.251	$-13.39^{+0.14}_{-0.15}$	$1.49^{+0.66}_{-0.57}$	$-13.35^{+0.09}_{-0.09}$	$0.86^{+0.40}_{-0.33}$
J1824-2452A	2626	13.80	2.190	$-12.56^{+0.13}_{-0.12}$	$3.61^{+0.41}_{-0.39}$	$-12.18^{+0.11}_{-0.10}$	$1.64^{+0.46}_{-0.59}$
J1832-0836	326	5.40	1.430	$-16.47^{+2.63}_{-3.09}$	$3.66^{+2.33}_{-2.52}$	$-13.07^{+0.24}_{-0.63}$	$3.77^{+2.00}_{-1.05}$
J1857+0943	3840	14.21	5.564	$-14.76^{+0.74}_{-0.50}$	$5.75^{+0.91}_{-1.53}$	$-13.40^{+0.20}_{-0.25}$	$2.66^{+0.83}_{-0.67}$
J1909-3744	14627	14.21	0.672	$-13.60^{+0.13}_{-0.12}$	$1.60^{+0.43}_{-0.46}$	$-13.48^{+0.09}_{-0.08}$	$0.69^{+0.38}_{-0.35}$
J1939+2134	4941	14.09	0.468	$-14.38^{+0.22}_{-0.18}$	$6.24^{+0.49}_{-0.62}$	$-11.59^{+0.07}_{-0.07}$	$0.13^{+0.19}_{-0.10}$
J2124-3358	4941	14.21	8.863	$-14.79^{+0.82}_{-0.67}$	$5.07^{+1.37}_{-1.97}$	$-13.35^{+0.18}_{-0.33}$	$0.95^{+1.11}_{-0.66}$
J2129-5721	2879	13.88	3.496	$-15.48^{+1.92}_{-3.54}$	$2.91^{+2.29}_{-1.83}$	$-13.31^{+0.13}_{-0.14}$	$1.07^{+0.65}_{-0.65}$
J2145-0750	6867	14.09	5.086	$-12.82^{+0.10}_{-0.11}$	$0.62^{+0.50}_{-0.40}$	$-13.33^{+0.14}_{-0.16}$	$1.38^{+0.54}_{-0.55}$
J2241-5236	5224	8.20	0.830	$-13.40^{+0.09}_{-0.08}$	$0.44^{+0.40}_{-0.30}$	$-13.79^{+0.10}_{-0.10}$	$1.42^{+0.61}_{-0.59}$

脉冲到达时间 (TOA)



Pulsar Modeling

```

PSRJ      J0030+0451
RAJ       00:30:27.4299630      1  0.00000000083327092134
DECJ      +04:51:39.75230       1  0.00000000193016085164
F0        205.53069608827312545  1  1.6735454617113885805e-13
F1        -4.3060388399134177208e-16 1  2.0847319452591396919e-21
PEPOCH    53000
POSEPOCH  53000
DMEPOCH   53000
PMRA      -4.0541352583640798551  1  0.06006537664217530270
PMDEC     -5.0337686500180439013  1  0.14002511698705866205
PX        4.0229124332613435578  1  0.02065704842394362750
EPHVER    5
CLK       UNCORR
MODE 1
EPHEM     DE414
DM        1 1 0
DM1       0 1 0
DM2       0 1 0
    
```

Right ascension, RA (J2000)
 Declination, DEC (J2000)
 Proper motion in RA (mas yr^{-1})
 Proper motion in DEC (mas yr^{-1})
 Spin frequency, f (s^{-1})
 \dot{f} (s^{-2})
 Parallax, π (mas)
 Dispersion measure, DM ($\text{cm}^{-3} \text{ pc}$)
 $\dot{\text{DM}}$ ($\text{cm}^{-3} \text{ pc yr}^{-1}$)
 $\ddot{\text{DM}}$ ($\text{cm}^{-3} \text{ pc yr}^{-2}$)
 Binary model
 Orbital period, P_b (d)
 Epoch of periastron, T_0 (MJD)
 Projected semi-major axis, x (lt-s)
 Longitude of periastron, ω_0 (deg)
 Eccentricity, e
 Sine of inclination, $\sin i$
 Companion mass, m_c (M_\odot)
 Derivative of P_b , \dot{P}_b
 Periastron advance $\dot{\omega}_0$ (deg yr^{-1})
 Epoch of ascending node, T_{asc} (MJD)

Noise Model

White noise (irrelevant to signal): from device, pulsar timing template

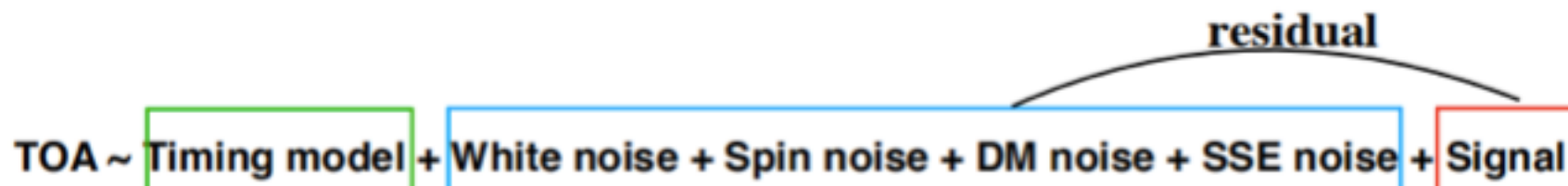
Red noise (relevant) : pulsar rotation noise, from propagation

Turbulence in the solar system: from big planet, etc

Noise from target sources: plasma cloud between pulsar and earth

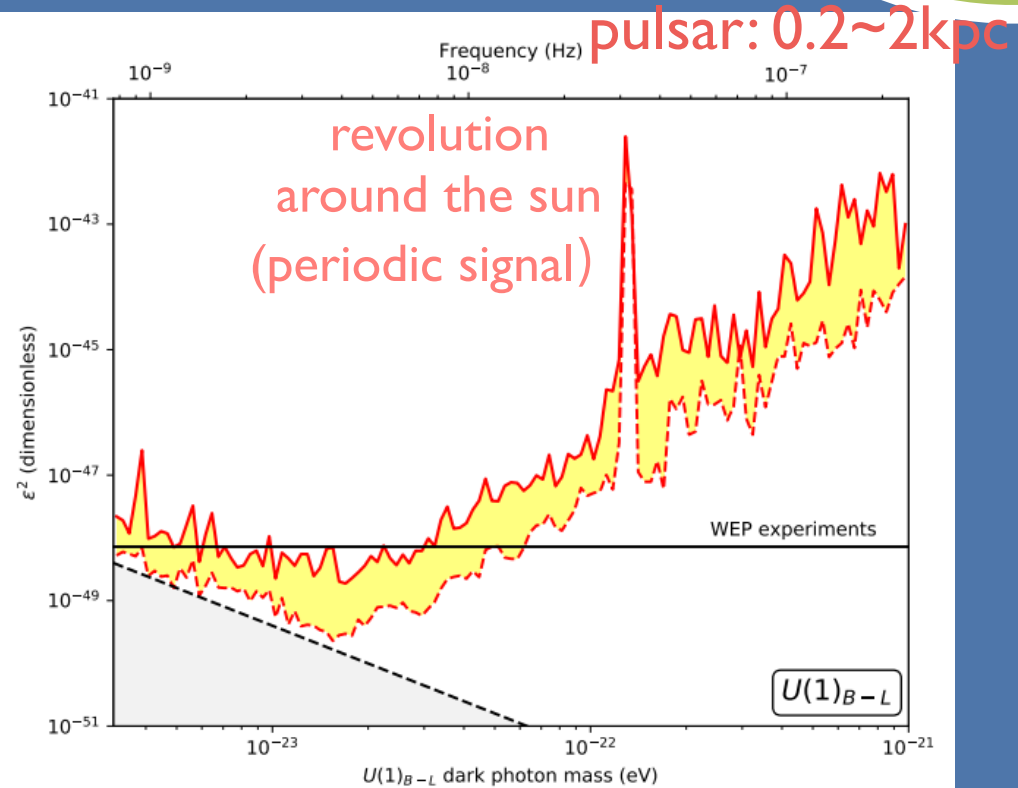
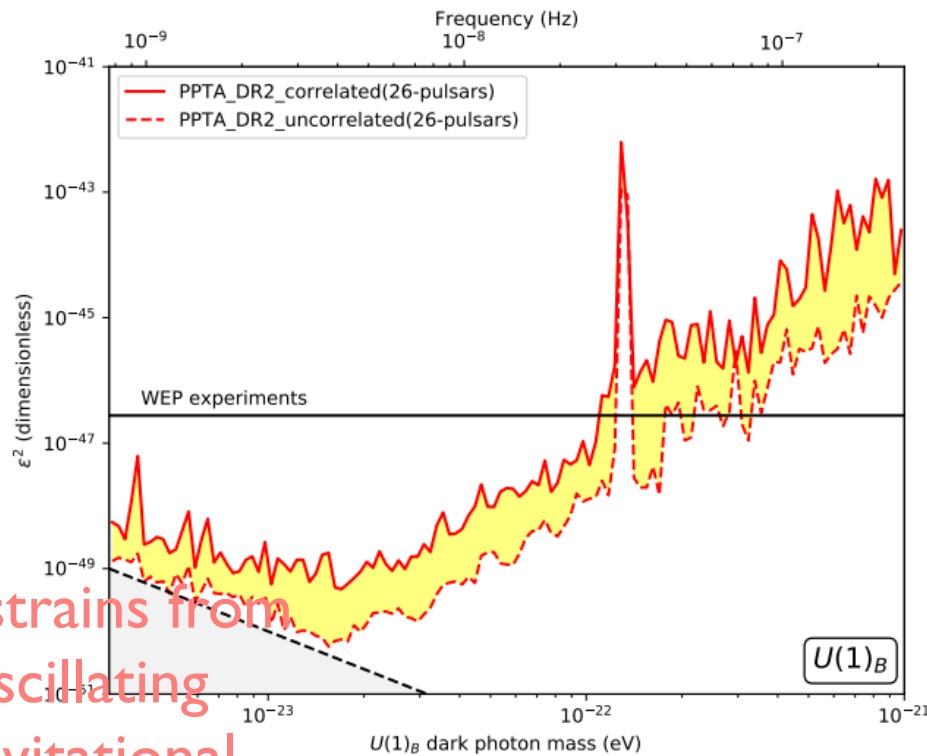
$$\text{TOA} \sim \text{Timing model} + \text{White noise} + \text{Spin noise} + \text{DM noise} + \text{SSE noise} + \text{Signal}$$

residual

The diagram shows the equation TOA ~ Timing model + White noise + Spin noise + DM noise + SSE noise + Signal. A blue bracket is drawn above the terms 'White noise + Spin noise + DM noise + SSE noise', and the word 'residual' is written above the bracket.

Parke PTA preliminary

fully correlated (lower) or uncorrelated (upper) DPDM polarization



pulsar: 0.2~2kpc

Constrains from
oscillating
gravitational
potential

J. Shu., X. Xiao, Z-j. Xia, Q. Yuan, Y. Zhao, X-j. Zhu, with PPTA collaboration

Will be the best in the world for certain mass range

A decorative graphic consisting of several circles of different colors (orange, green, blue) and white outlines, connected by thin white lines, set against a dark blue background. The circles are arranged in a way that they appear to be part of a larger, abstract structure.

Probing Axions with Event Horizon Telescope Polarimetric Measurements

Y-f. Chen, [J. Shu.](#), X. Xiao, Q. Yuan, Y. Zhao,
Phys.Rev.Lett. 124 (2020) 061102

Theory motivation

Strong CP problem

$$\frac{(\theta - \arg \det M_q) \frac{\alpha_s}{8\pi} G\tilde{G}}{-\pi \leq \theta \leq +\pi}$$

$$< 10^{-11}$$

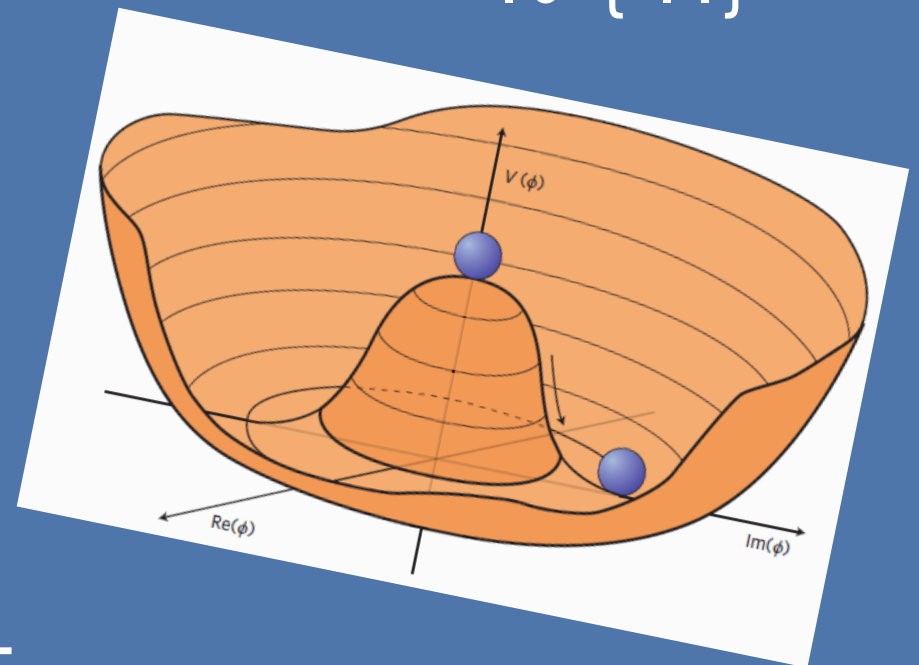
Induced axion fields

misalignment



PQ symmetry soft explicit
broken at high scale f

pNGB naturally very light



Why axion?

Big problems of particle physics & Cosmology

- Strong CP problem
- The identity of dark matter misalignment mechanism,
non-thermal DM
- Gauge hierarchy problem, the origin of EWSB relaxion
- Baryogenesis
- Inflation
- Cosmological Constant Problem

Search of axion

How to search axion?

Axion-couplings:

● Axion-photon

ADMX

LIGO, pulsar, etc

CAST

● Axion-gluon

QCD phase transition

CASPEr

Many other observations, etc

Axion like particle

Axion induce birefringent effect:

$$\mathcal{L} = -\frac{1}{4}F_{\mu\nu}F^{\mu\nu} - \frac{1}{2}g_{a\gamma}aF_{\mu\nu}\tilde{F}^{\mu\nu} - \frac{1}{2}\nabla^\mu a\nabla_\mu a - V(a),$$

$$\nabla \cdot \mathbf{E} = g \nabla \varphi \cdot \mathbf{B}, \quad \nabla \times \mathbf{E} + \frac{\partial \mathbf{B}}{\partial t} = 0,$$

$$\nabla \times \mathbf{B} - \frac{\partial \mathbf{E}}{\partial t} = g \left(\mathbf{E} \times \nabla \varphi - \mathbf{B} \frac{\partial \varphi}{\partial t} \right),$$

$$\nabla \cdot \mathbf{B} = 0,$$

$$\square \varphi = \frac{\partial^2 \varphi}{\partial t^2} - \nabla^2 \varphi = -g \mathbf{E} \cdot \mathbf{B}.$$

The condensation of a CP-odd particle distinguishes +/- helicities of a photon

Maxell equation
with axion source

Birefringent effect

Axion induced birefringent effect

$$\square A_{\pm} = \pm 2ig_{a\gamma}[\partial_z a \dot{A}_{\pm} - \dot{a} \partial_z A_{\pm}],$$

$$\omega_{\pm} \approx k_{\pm} \pm \frac{1}{2}g \left(\frac{\partial \varphi}{\partial t} + \nabla \varphi \cdot \frac{\mathbf{k}}{k} \right)$$

different phase velocities
for +/- helicities

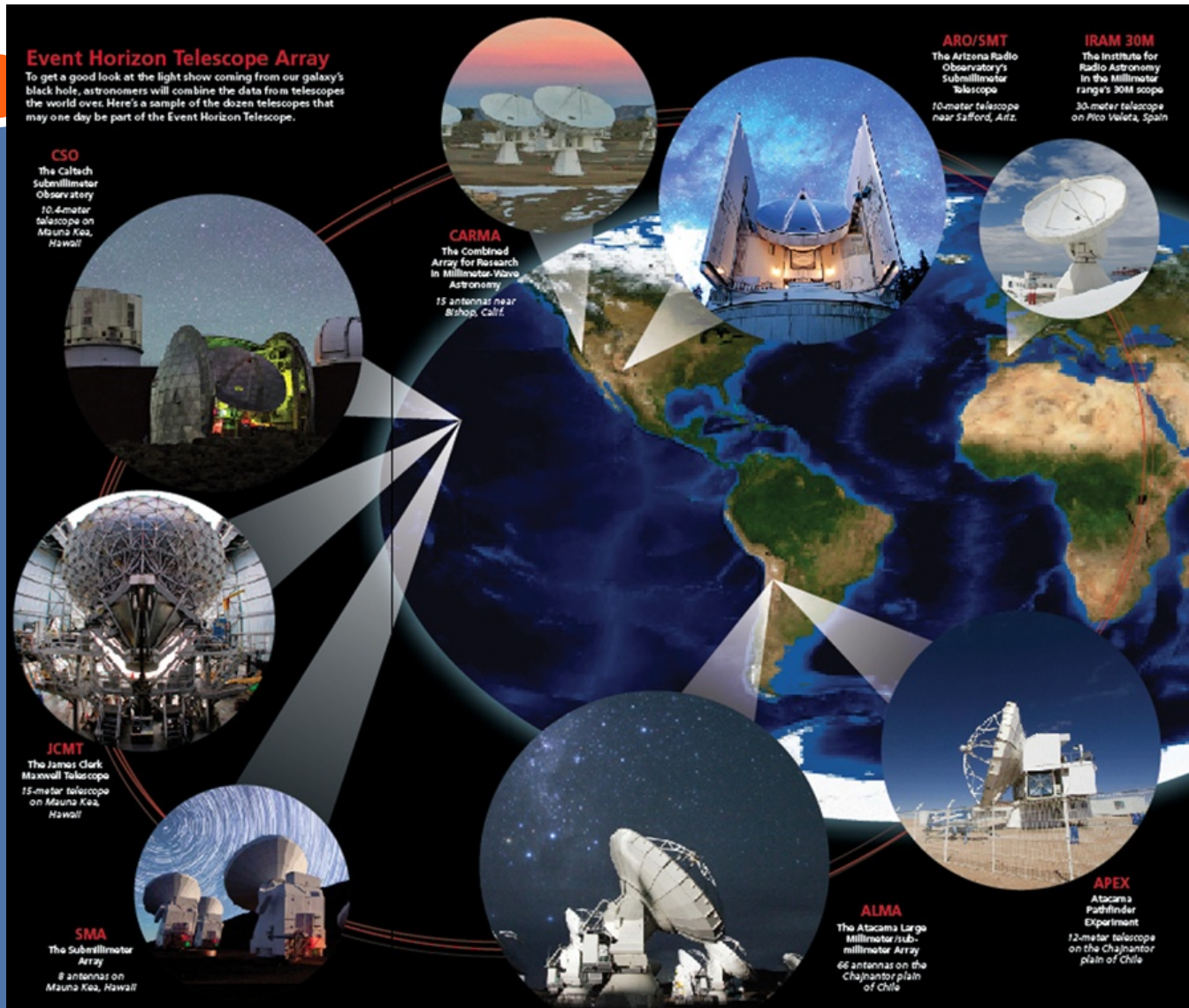
For linearly polarized photons

$$\begin{aligned} \Delta \Theta &= g_{a\gamma} \Delta a(t_{\text{obs}}, \mathbf{x}_{\text{obs}}; t_{\text{emit}}, \mathbf{x}_{\text{emit}}) \\ &= g_{a\gamma} \int_{\text{emit}}^{\text{obs}} ds n^{\mu} \partial_{\mu} a \\ &= g_{a\gamma} [a(t_{\text{obs}}, \mathbf{x}_{\text{obs}}) - a(t_{\text{emit}}, \mathbf{x}_{\text{emit}})], \end{aligned}$$

Measure the change of
the position angle:

Requires polarimetric
measurements

Event Horizon Telescope



mm telescope array
at radio frequency
around the Earth

mm wavelength radio
telescope particularly
good for astro-astro-
polarimetric
measurements

Farady rotation:
position angle
around $O(I)$

Imagine of M87*

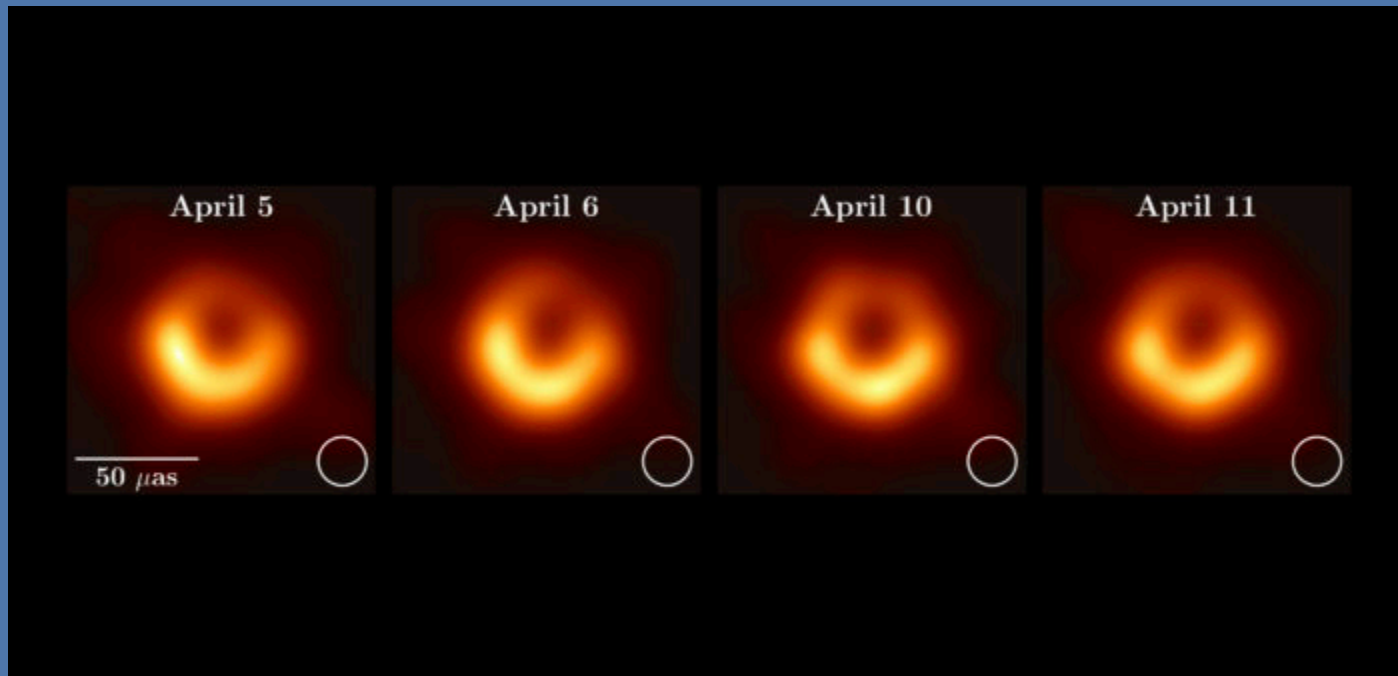


Image of the supermassive black hole at the center of the elliptical galaxy M87, for four different days.

The image of the ring is around **5 horizon distance**

BH measured and EHT

Blackhole measured:

M87*: 16 Mpc, 10^9 solar mass
 10^{13} m, 10^{-20} eV
 10^5 s, $a=0.99$

Excellent angular resolutions:

Sgr A*: 8 kpc, 10^6 solar mass
 10^{10} m, 10^{-17} eV
 100 s, $a=?$

20 micro as

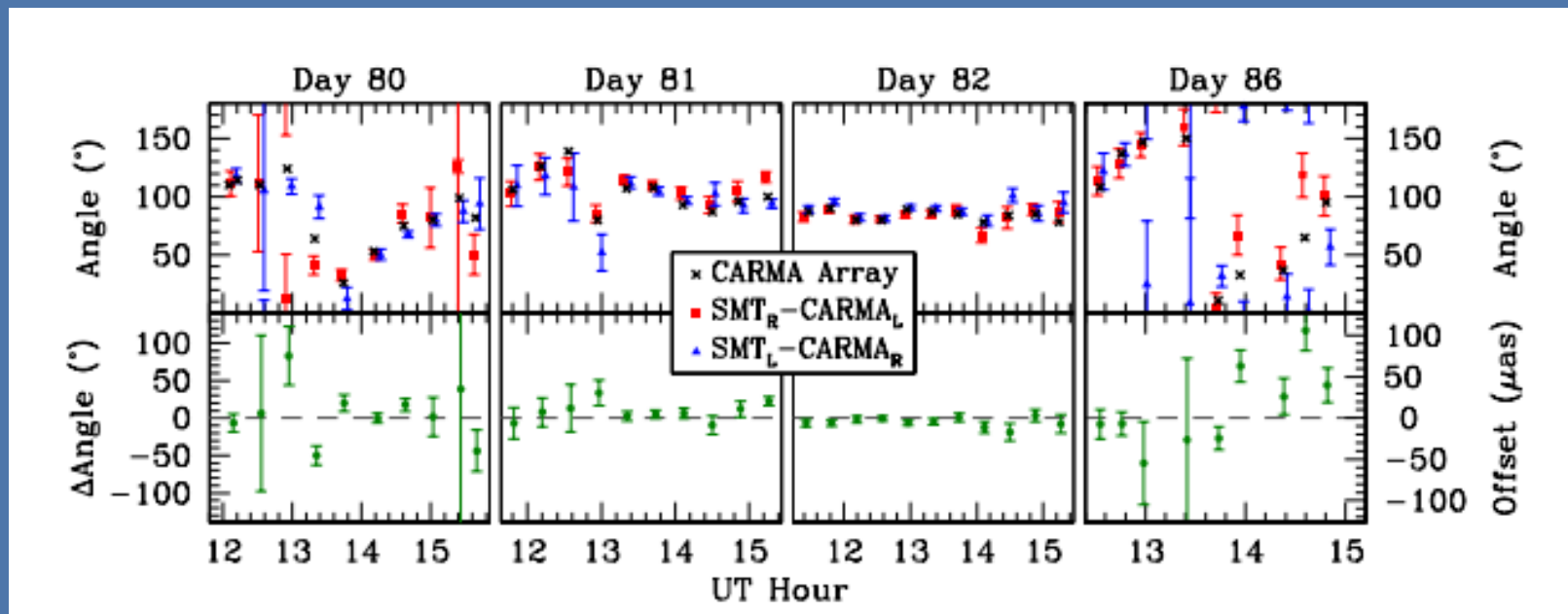
resolve features: smaller than BH size (1/3?)

SMBH	M	a_J	μ range	μ for $\alpha = 0.4$	τ_a	τ_{SR}
M87*	$6.5 \times 10^9 M_\odot$	0.99	$2.1 \times (10^{-21} \sim 10^{-20})$ eV	8.2×10^{-21} eV	5.0×10^5 s	$> 1.5 \times 10^{12}$ s
Sgr A*	$4.3 \times 10^6 M_\odot$	—	$3.1 \times (10^{-18} \sim 10^{-17})$ eV	1.2×10^{-17} eV	3.3×10^2 s	$> 1.0 \times 10^9$ s

TABLE I: Typical parameters of the axion superradiance of the two SMBHs, M87* and Sgr A*.

More on EHT measurements

Accretion disk around SMBH gives linearly polarized radiation
Millimeter wavelength: optimal for position angle measurements

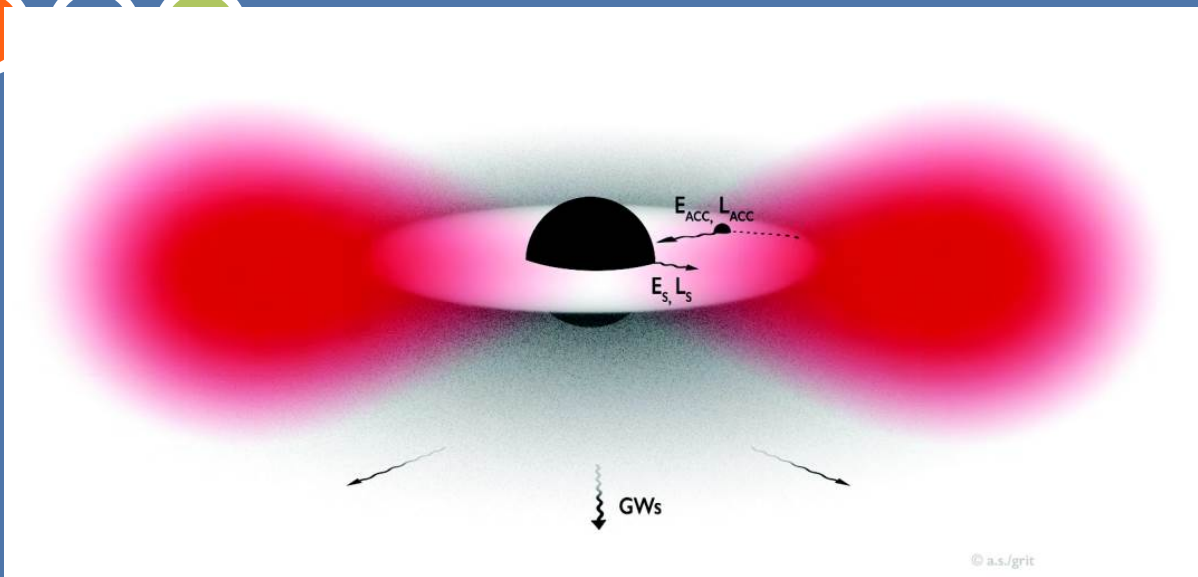


No spatial resolution

• M. D. Johnson et al., Science 350, no. 6265, 1242 (2015)

A subset of EHT has achieved at a precision of 3 degree!

BH superradiance



Superradiance condition

$$\omega < \omega_c = \frac{a_j m}{2r_+}$$

a rapidly rotating black hole loses:
energy + angular momentum

axion cloud will be produced around BH

SR takes efficiently for the mass range

$$\frac{r_g}{\lambda_C} = \mu M \equiv \alpha \in (0.1, 1),$$

energy in axion cloud can be comparable to BH mass!

BH superradiance

Axion cloud: Scalars in the Kerr backgrounds

Very similar to the hydrogen solution (non-relativistic limit):

$$a(x^\mu) = e^{-i\omega t} e^{im\phi} S_{lm}(\theta) R_{lm}(r)$$

$$\alpha \equiv \mu M$$

reduce to Y_{lm} in spherical non-relativistic limit

$$\text{Re}(\omega) \simeq \left(1 - \frac{\alpha^2}{2\bar{n}^2}\right) \mu$$

Imaginary part gives you the super-radiation

Axion cloud populates more efficiently at lower ℓ -mode.

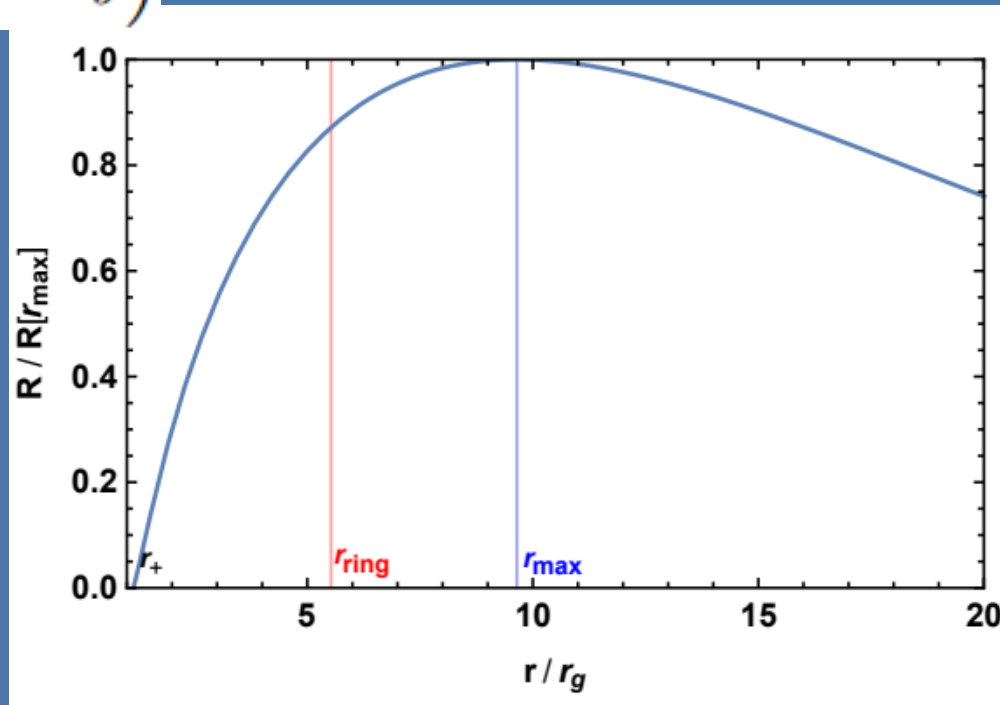
$m=\ell$ mode is more efficient than other m -levels.

BH superradiance

Spatial distribution:

$$r_{\pm} = r_g \left(1 \pm \sqrt{1 - a_J^2} \right)$$

The ring from EHT has a **radius comparable to the peaking radius** of the axion cloud



Axion cloud solution

Axion Lagrangian including self-interaction:

$$S = \int d^4x \sqrt{-g} \left[-\frac{1}{2} (\nabla a)^2 - \mu^2 f_a^2 \left(1 - \cos \frac{a}{f_a} \right) \right]$$

K-G equation in the Kerr backgrounds

take

$$a = \frac{1}{\sqrt{2\mu}} (e^{-i\mu t} \psi + e^{i\mu t} \psi^*)$$

slow varying function

gravitational potential

$$S_{\text{NR}} = \int d^4x \left(i\psi^* \partial_t \psi - \frac{1}{2\mu} \partial_i \psi \partial_i \psi^* - \frac{\alpha}{r} \psi^* \psi + \frac{(\psi^* \psi)^2}{16f_a^2} \right)$$

self-interacting potential

Non-linear region

axion self-interaction becomes important when

gravitational potential \sim self-interacting potential

$$\frac{\alpha}{r} \simeq \frac{\mu a_0^2}{4f_a^2}$$

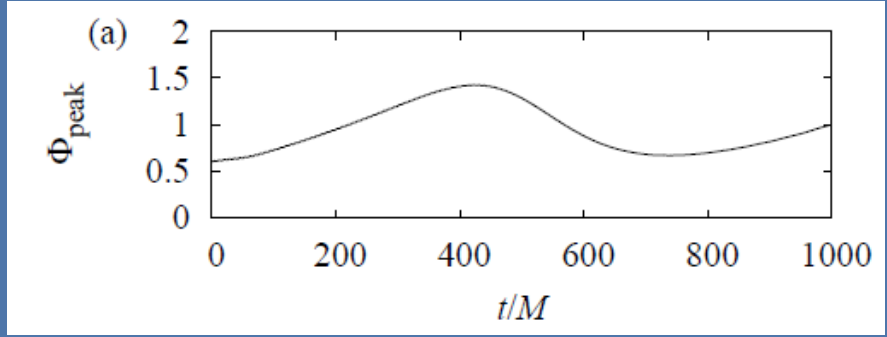
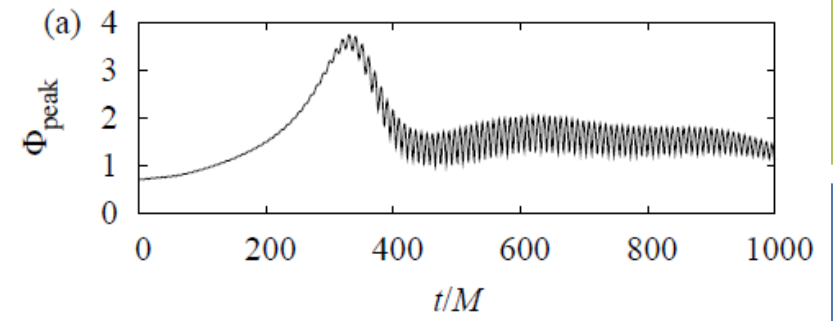
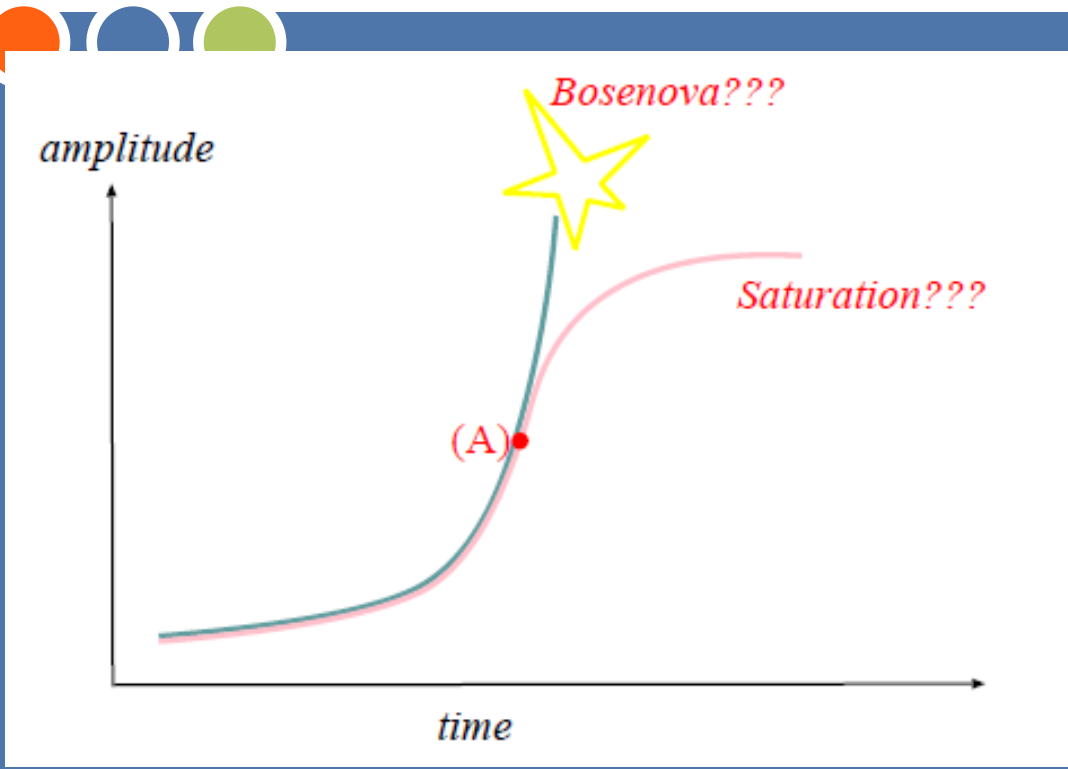
Two possible consequences:

bosenova: a drastic process which explodes away axion cloud

steady axion outflow to infinity

numerical simulation has been performed:

Bosenova



In either scenario, the amplitude of the axion cloud remains $O(1)$ of its maximal value for most of the time

$$\frac{a}{f_a} \sim O(1)$$

The axion cloud stays after bosenova

Position angle change

Using $a_0 \approx f_a$ and $\omega \approx \mu$

Ignore axion density at earth

$$\Delta\Theta_{\max} \simeq -bg_{a\gamma}f_a \cos[\mu t_{\text{emit}} + \beta(|\mathbf{x}_{\text{emit}}| = r_{\max})],$$

$$b \equiv a_{\max}/f_a$$

$$\Delta\Theta(t, r, \theta, \phi) \approx -\frac{bg_{a\gamma}f_a R_{11}(r)}{R_{11}(r_{\max})} \sin\theta \cos[\omega t - m\phi]. \quad (17)$$

Require both time and spatial resolution

additional loop suppression to translate f_a to axion-photon coupling

$$g_{a\gamma} \equiv \frac{c}{2\pi f_a} \equiv \frac{c_\gamma \alpha_{em}}{4\pi f_a},$$

fermion loop

$$c_\gamma \sim NQ^2.$$

clockwork

$$c_\gamma \sim 2Q^2 q^{N-M}.$$

Large

Polarmetric measurements



Requirements:

Concentration of axion: oscillating background fields

Stable (position angle) polarized source

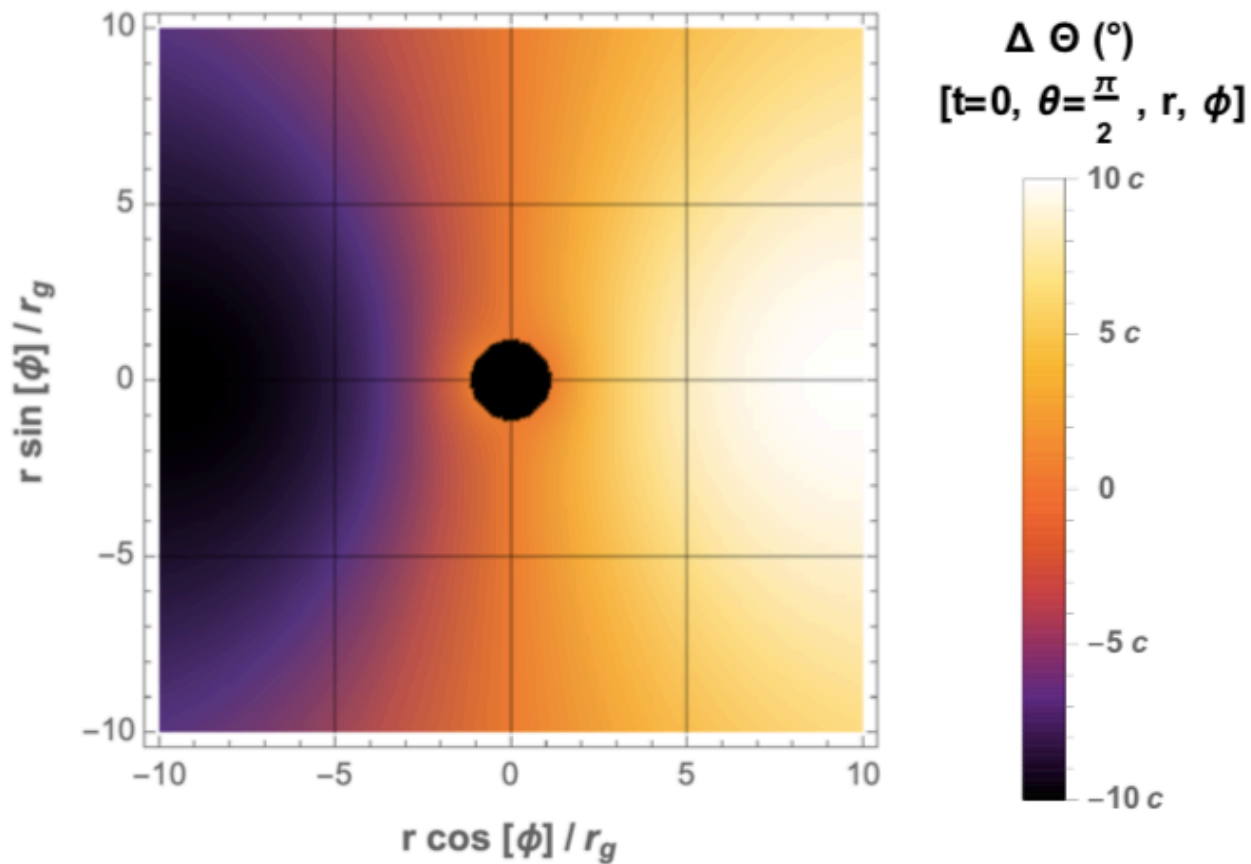
Search for:

Position angle **oscillate with time**

Position angle **oscillate with spatial distributions** (extended source)

Polarmetric measurements at EHT from the axion cloud!

Position angle change



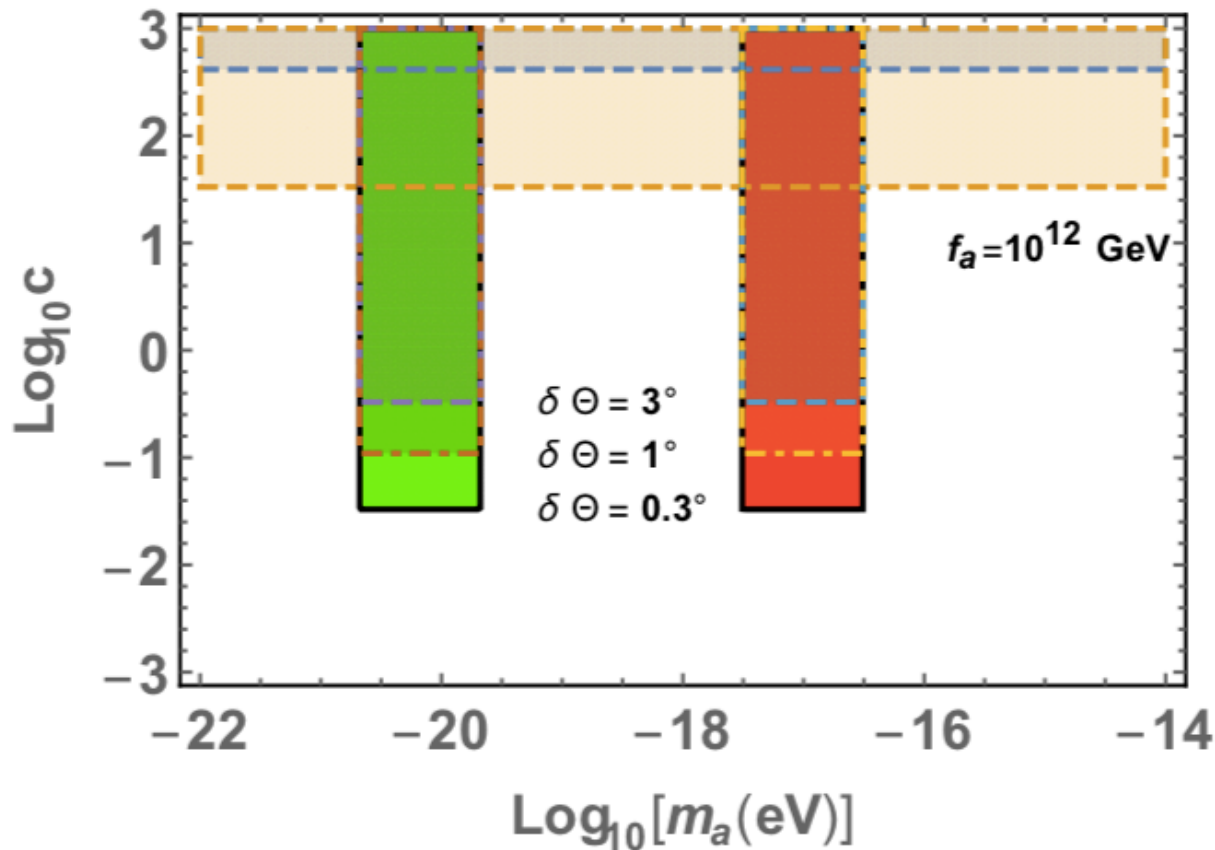
- temporal dependence for a fixed position

- spatial dependence for a fixed time

FIG. 2: $\Delta\Theta(t = 0, \theta = \pi/2, r, \phi)$ viewed along the rotating axis of the black hole. The amplitude of oscillation is around $8c^\circ$ at r_{ring} for $l = 1$, $m = 1$, $\alpha = 0.4$, and $a_J = 0.99$. The region of $r < r_+$ is masked.

Y-f. Chen, [J. Shu.](#), X. Xiao, Q. Yuan, Y. Zhao, Phys.Rev.Lett. 124 (2020) 061102

Expected Limit

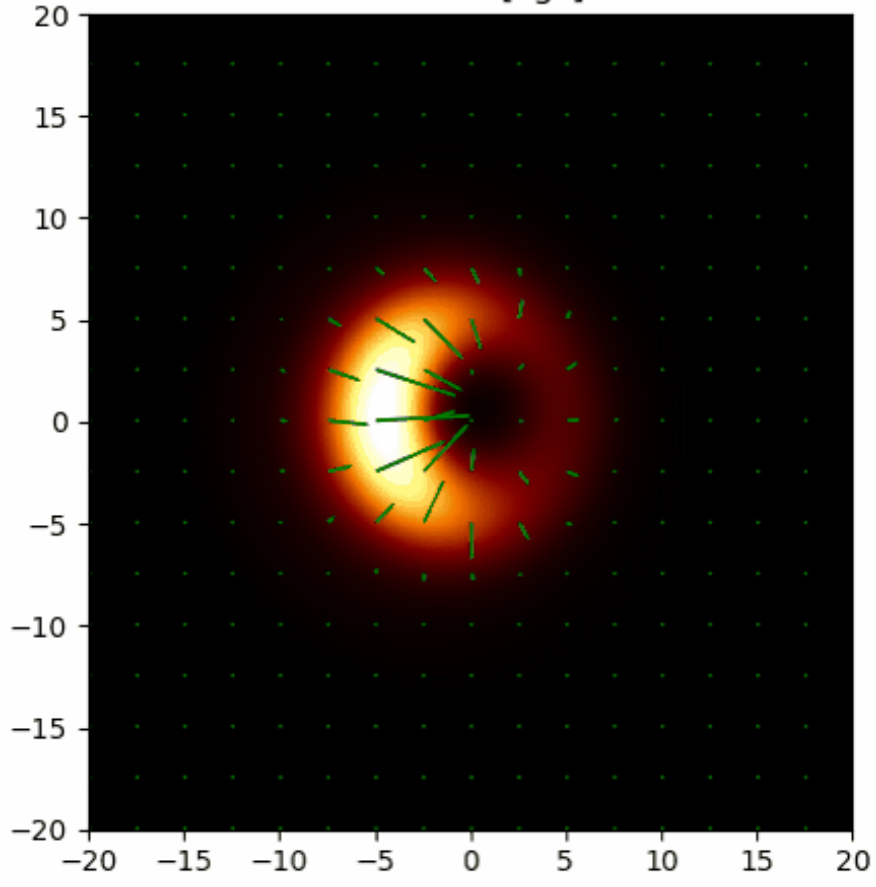


Constrain the dimensionless coupling with respect to f_a

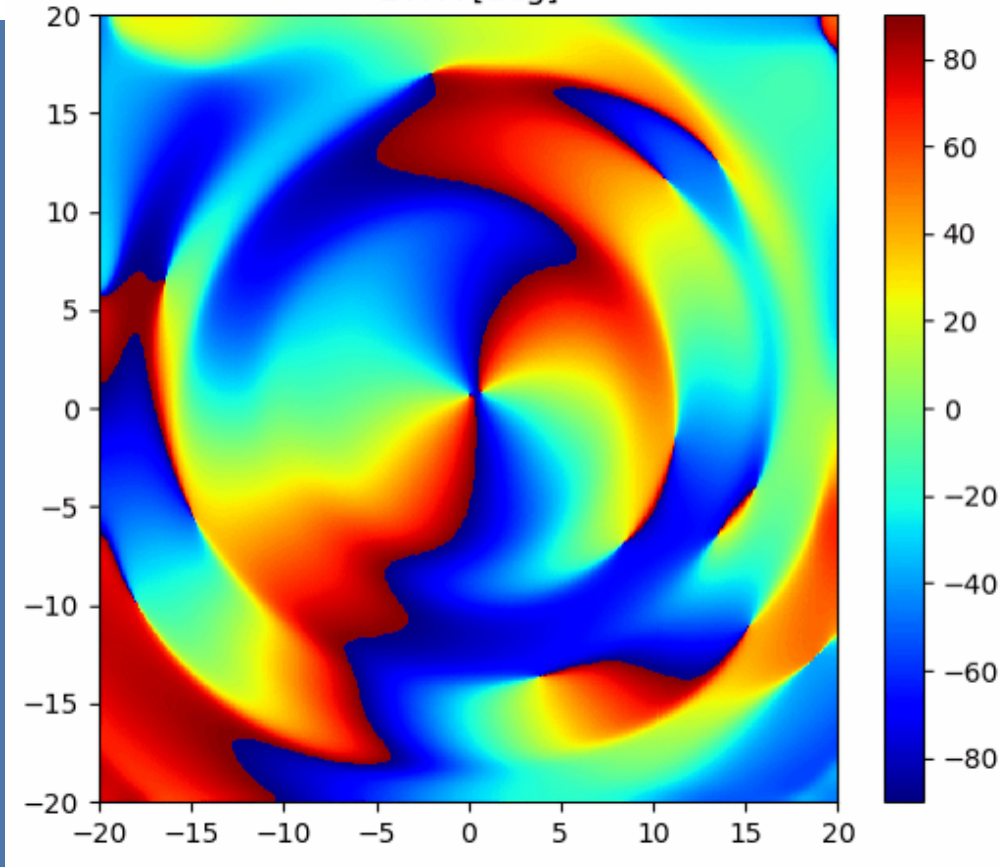
CAST SN1987A M87* Sgr A*

Expected Limit

Stokes I [cgs]



EVPA [deg]



Real simulation layered with accretion disk backgrounds

Y-f. Chen, [J. Shu.](#), X. Xiao, Q. Yuan, Y. Zhao, collaboration with EHT

Summary

Ultra-light particles can form an oscillating background, cause extra forces on the observer and the objects we observe

Oscillating Velocity change: observed by Gaia

Arriving Time (pulse) change: observed by PTA **Real data/better sensitivity**

Supermassive Black holes provides excellent probes to search for axion!

A dense axion cloud can build up near by SMBHs.

Position angles varies when traveling through the axion cloud

Probe the existence of axion clouds by EHT.

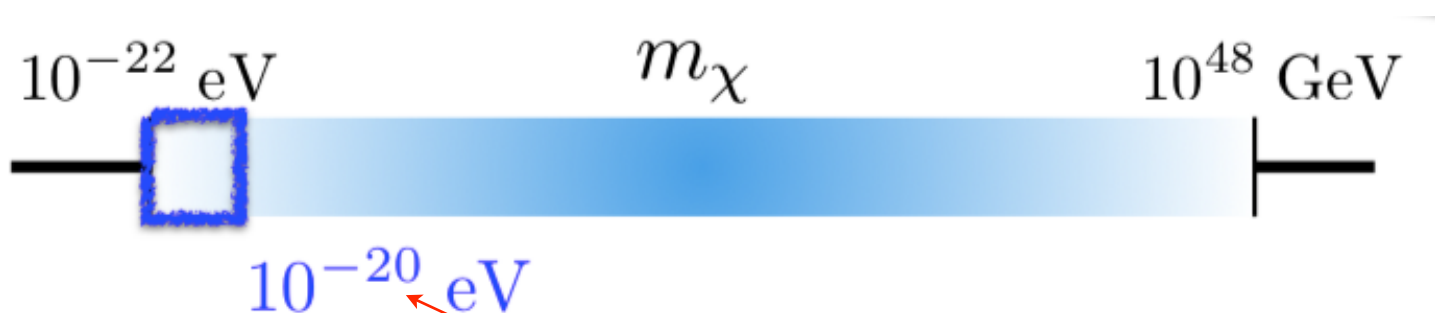
Different than BH spin measurement. **(Nonlinear region)**

Different than other experiment. **(dimensionless coupling)**

A decorative graphic on a blue background. It features a central white rounded rectangle containing the text. To the left of the rectangle is a large orange circle, and below it is a smaller green circle. To the right of the rectangle is a green circle above a larger blue circle. A white outline of a circle is positioned above the rectangle, and a white line connects the orange circle to this outline. The text is in a bold, red, sans-serif font.

Detecting axion through quantum sensors

超轻暗物质轴子的探测



Hu, Barkana, Gruzinov '00
Hui, Ostriker, Tremaine, Witten '17

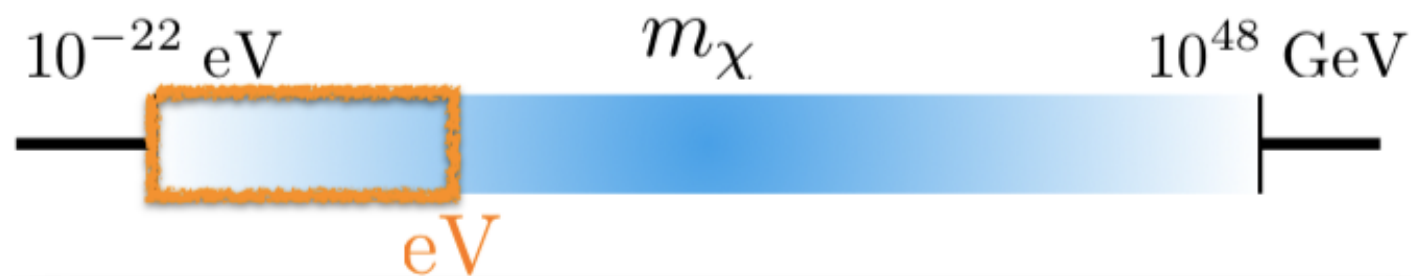
$$10^{10} M_\odot \left(\frac{10^{-22} \text{ eV}}{m} \right)^{4/3}$$

宇宙早期生成非相对论性的轴子(冷暗物质)

质量极轻，德布罗意波长极大(小星系尺度)，波动性，可以用来解释小星系暗物质缺乏问题

波动性的暗物质

超轻暗物质轴子的探测



- 解决了强CP问题。
- String理论，额外维度预言了大量轴子的存在。解决了强CP问题。
- 可以用于其他在重大问题，比如暴涨，宇宙早期正反物质不对称性，电弱对称性破缺，规范等级度问题等等。

一般性的轴子探测（更广泛的质量范围）

宇宙轴子能量动量分布

$$a(t) = \frac{\sqrt{2\rho_{\text{DM}}}}{m_a} \cos(m_a t + \phi)$$

Frequency: $\omega_a \simeq \text{GHz} \frac{m_a}{10^{-6} \text{ eV}}$

Coherence: $\tau_a \simeq \text{ms} \frac{10^{-6} \text{ eV}}{m_a}$

Max Exp. Size: $\lambda_a \simeq 200 \text{ m} \frac{10^{-6} \text{ eV}}{m_a}$

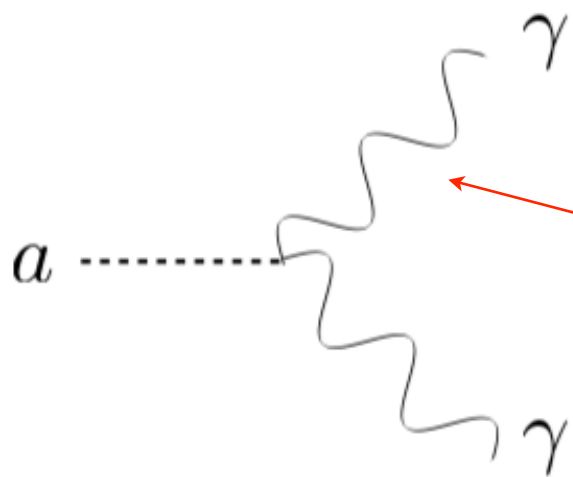
$$\tau_a \sim 1/m_a \langle v_{\text{DM}}^2 \rangle \sim Q_a/m_a \sim 10^6/m_a$$

能量分布 10^{-6} ，对
应于 Q 大了没用

$$\lambda_a \sim 1/m_a \sqrt{\langle v_{\text{DM}}^2 \rangle} \sim 10^3/m_a$$

动量分布 10^{-3}

轴子实验室探测



(反)Primakoff 现象

一般性的轴子
探测 (更广泛
的质量范围)

$$\nabla \times \mathbf{B} \simeq \partial_t \mathbf{E} + \mathbf{J} + \underline{g_{a\gamma\gamma} \mathbf{B} \partial_t a}$$

轴子背景场在有背景磁场的情况下会产生额外的变化电场

$$J_{\text{eff}}(t) \sim g_{a\gamma\gamma} B_0(t) \sqrt{\rho_{\text{DM}}} \cos m_a t$$

Resonant EM detection of axion dark matter

Cavity mode equation

Source: \mathbf{a}
(almost monochromatic)

$$\sum_n \left(\partial_t^2 + \frac{\omega_n}{Q_n} \partial_t + \omega_n^2 \right) \mathbf{E}_n = g_{a\gamma\gamma} \partial_t (\mathbf{B} \partial_t a)$$

Signal Mode: \mathbf{E}_n

Pump Mode: \mathbf{B}

- Traditional resonant detection matches axion mass with the resonant frequency by using a static B field.

$$\omega_1 \simeq m_a \quad \partial_t(\mathbf{B}) \simeq 0$$

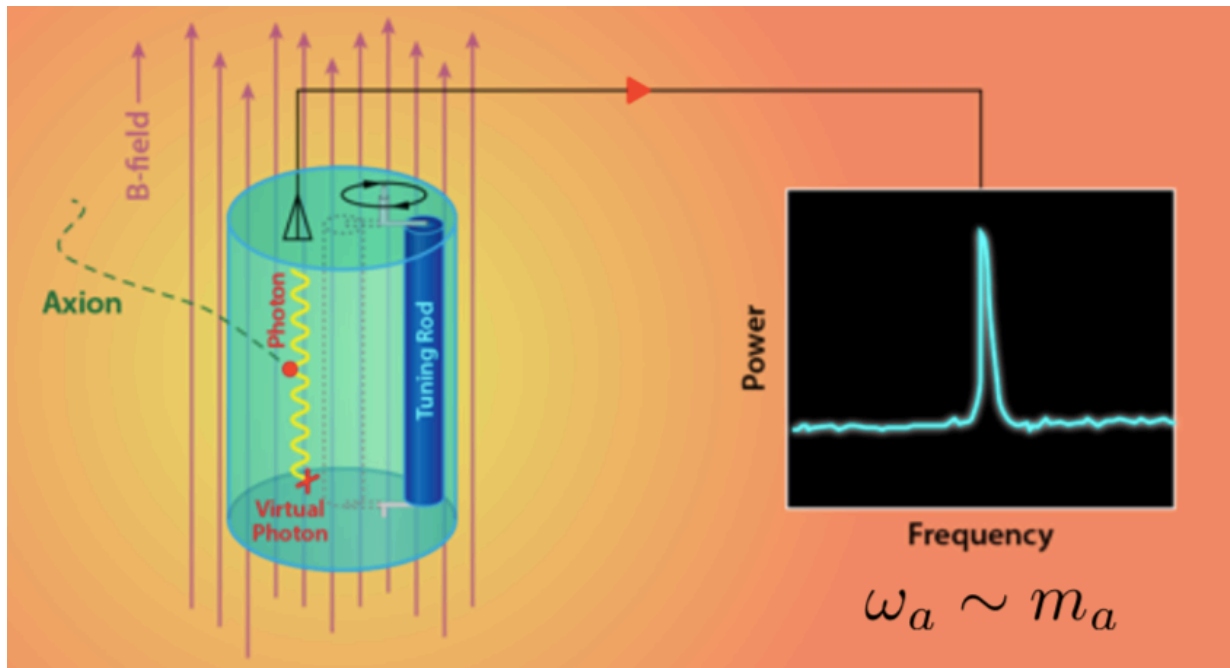
$$\left(\partial_t^2 + \frac{m_a}{Q_1} \partial_t + m_a^2 \right) \mathbf{E}_1 = g_{a\gamma\gamma} \mathbf{B} \sqrt{\rho_{\text{DM}}} m_a \cos m_a t$$

Cavity with static B field

$$\left(\partial_t^2 + \frac{m_a}{Q_1} \partial_t + m_a^2 \right) \mathbf{E}_1 \sim m_a \cos m_a t$$

$$Q_a \sim 10^6$$

$$m_a \sim \text{GHz} \sim 10^{-6} \text{ eV}$$



Cavity size \sim (axion mass)⁻¹

Signal power
decreases with axion mass

e.g. ADMX, HAYSTACK

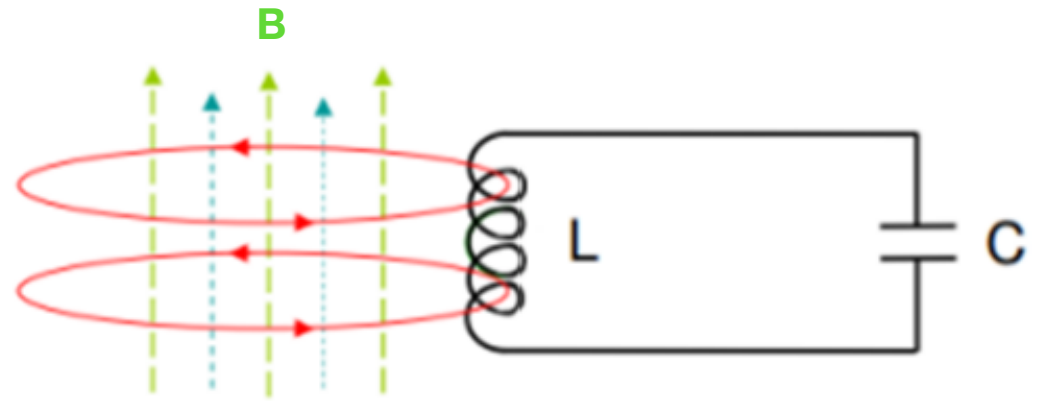
LC Circuit with static B field

- Resonant conversion happens when

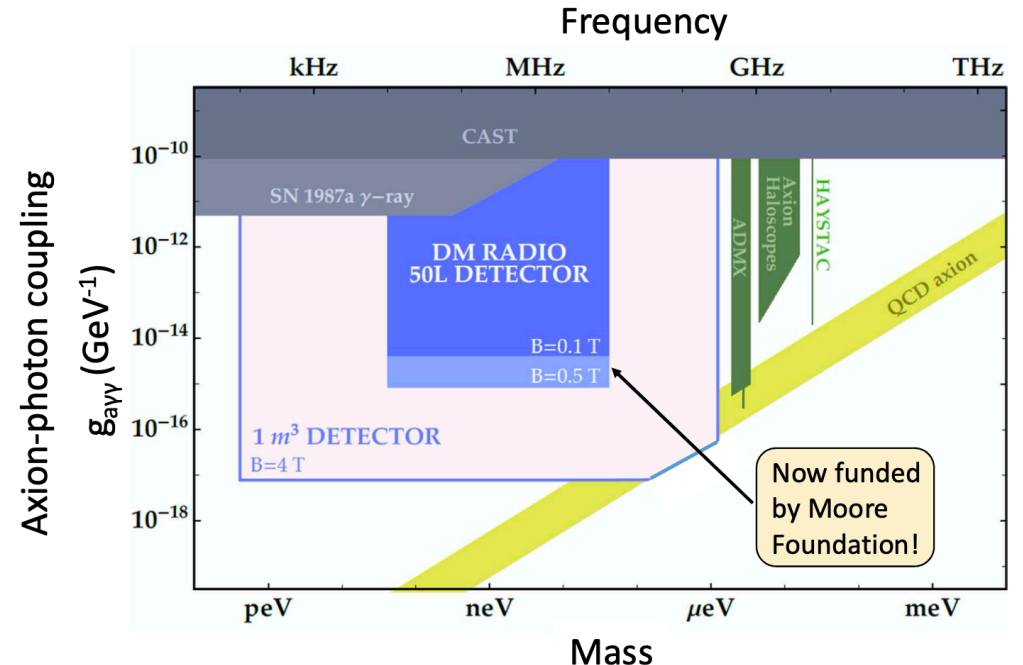
$$m_a = \omega = \frac{1}{\sqrt{LC}}$$

- Scan the mass from 100 Hz to 100 MHz by tuning the capacitor C

e.g. DM radio, ADMX-SLIC



DM Radio science: axions



Assumptions: $T=10$ mK, $Q=10^6$, 3.5 year integration time, quantum-limited readout

SRF with AC B field

Signal Mode: \mathbf{E}_1

Source: \mathbf{a}
(almost monochromatic)

$$\sum_n \left(\partial_t^2 + \frac{\omega_n}{Q_n} \partial_t + \omega_n^2 \right) \mathbf{E}_n = g_{a\gamma\gamma} \partial_t (\mathbf{B} \partial_t a)$$

Pump Mode: \mathbf{B}_0

Static \mathbf{B}_0 :

$$\omega_1 \simeq m_a \quad \partial_t(\mathbf{B}) \simeq 0$$

Oscillating \mathbf{B}_0 :

$$\omega_1 \simeq \omega_0 + m_a \quad \partial_t(\mathbf{B}) \simeq i\omega_0 \mathbf{B}$$

$$\mathbf{E}_1 \sim \frac{m_a g_{a\gamma\gamma} \sqrt{\rho_{\text{DM}}} \mathbf{B}}{m_a^2 - \omega_1^2 + i \frac{m_a \omega}{Q_1}}$$

$$\mathbf{E}_1 \sim \frac{\omega_0 g_{a\gamma\gamma} \sqrt{\rho_{\text{DM}}} \mathbf{B}}{(\omega_0 + m_a)^2 - \omega_1^2 + i \frac{(\omega_0 + m_a) \omega}{Q_1}}$$

Signal enhancement at low frequency $m_a \ll \omega_0$

SRF with AC B field

Signal Mode: \mathbf{E}_1

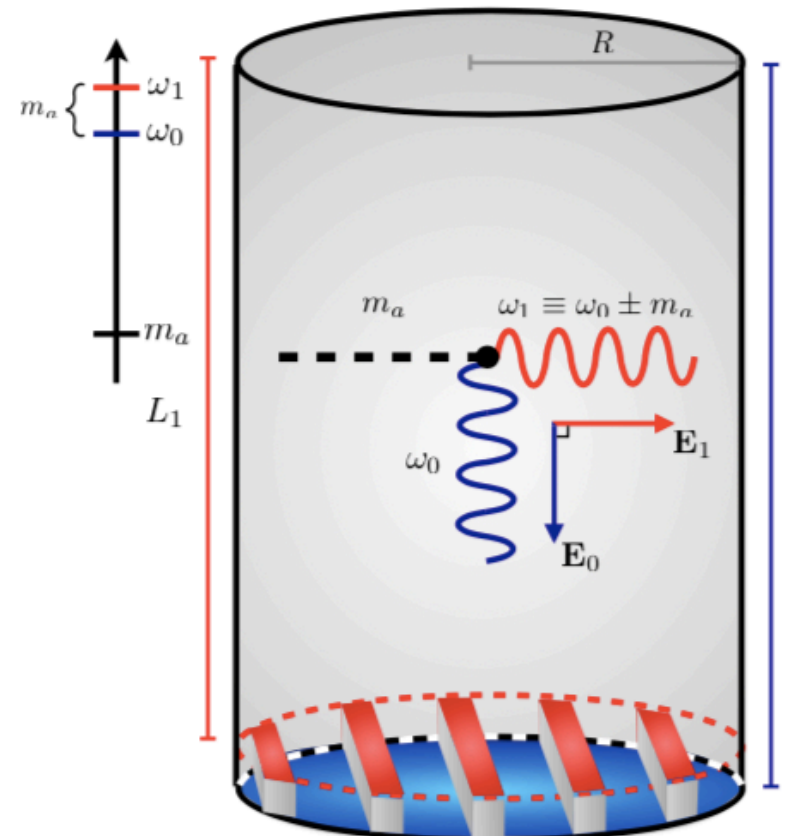
Source: \mathbf{a}
(almost monochromatic)

$$\sum_n \left(\partial_t^2 + \frac{\omega_n}{Q_n} \partial_t + \omega_n^2 \right) \mathbf{E}_n = g_a \gamma \partial_t (\mathbf{B} \partial_t a)$$

Pump Mode: \mathbf{B}_0

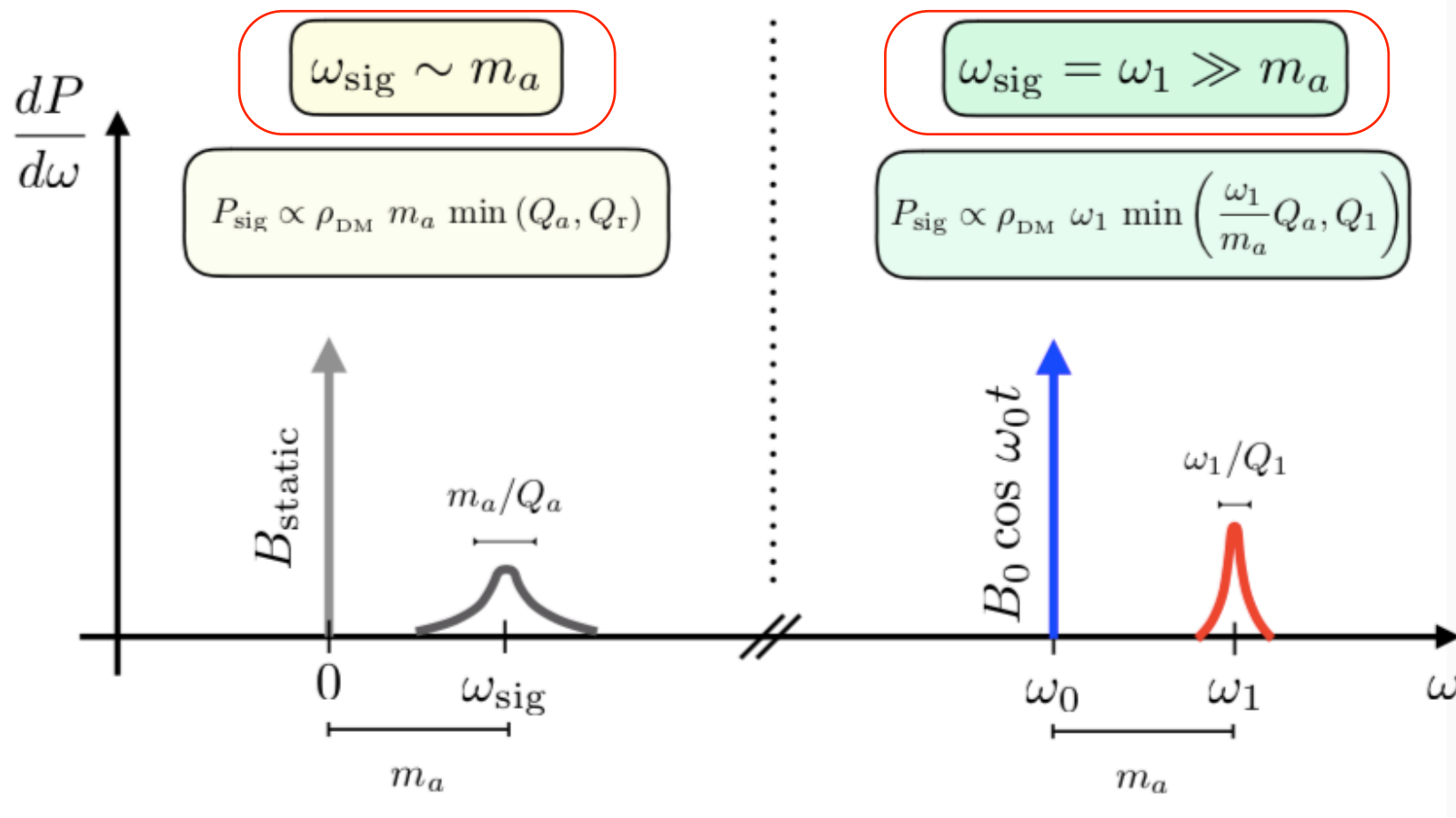
Oscillating \mathbf{B}_0 :

$$\omega_1 \simeq \omega_0 + m_a \quad \partial_t(\mathbf{B}) \simeq i\omega_0 \mathbf{B}$$



Scanning the axion mass by tuning the differences between two quasi-degenerate modes

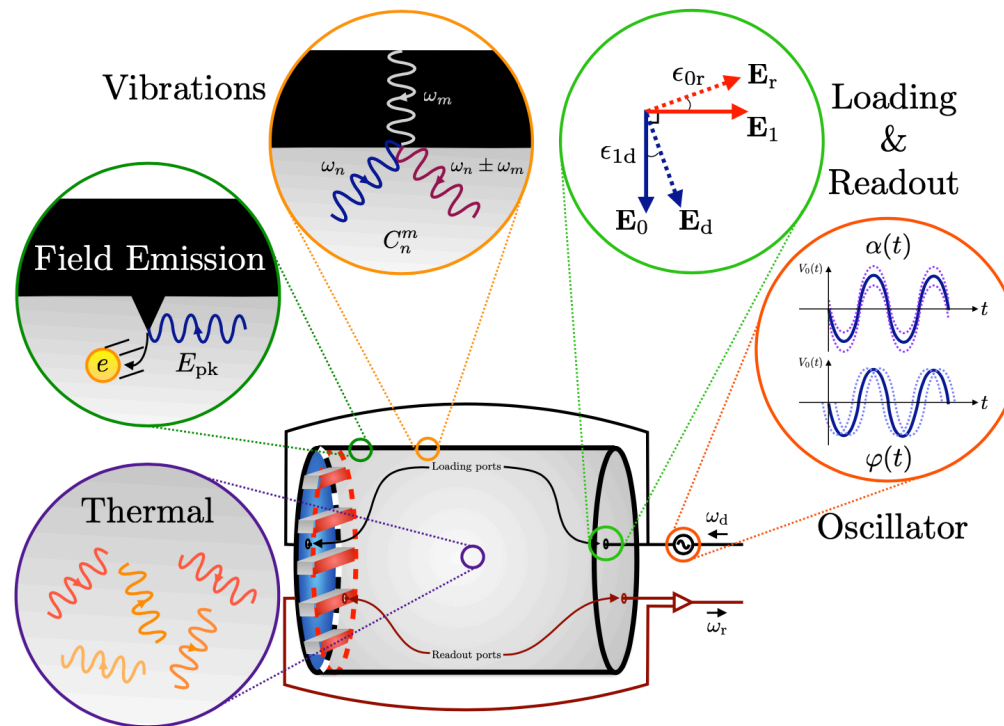
SRF with AC B field



Main differences: signal power

$$P_{\text{sig}}^{(r)} \sim \frac{\mathcal{E}_a^2}{R} \min\left(1, \frac{\tau_a}{\tau_r}\right) \sim \omega_{\text{sig}}^2 B_a^2 V \min(Q_r/\omega_{\text{sig}}, Q_a/m_a)$$

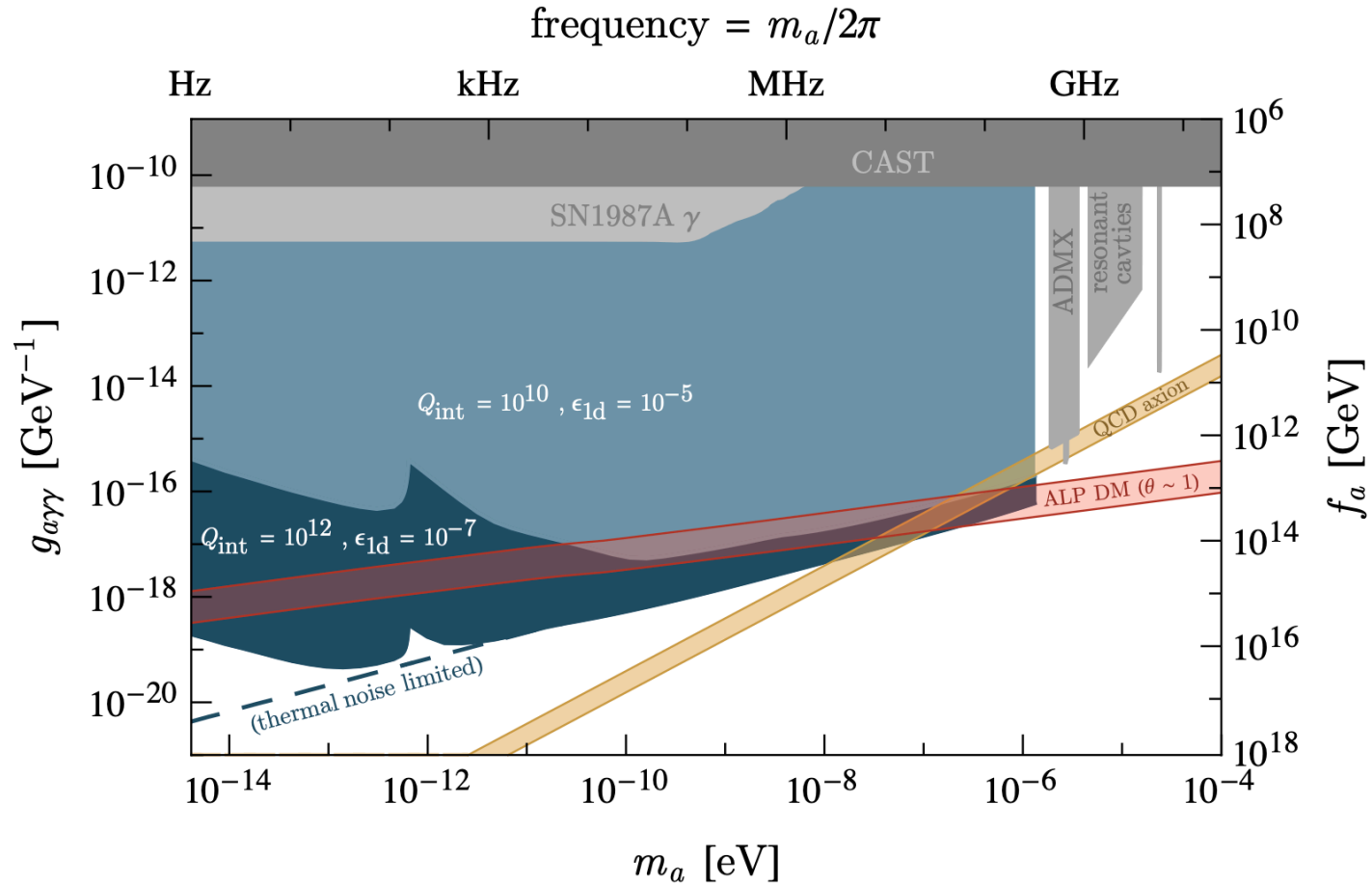
Main noise for SRF haloscope



Traditional noise: **thermal and readout**;

Transition from pumping mode due to geometric fluctuation:
phase noise, mechanical oscillation noise; (well-studied by pioneer work on ultra high frequency gravitational wave detection. [Class.Quant.Grav. 20 (2003) 3505-3522, gr-qc/ 0502054])

Physics Reach



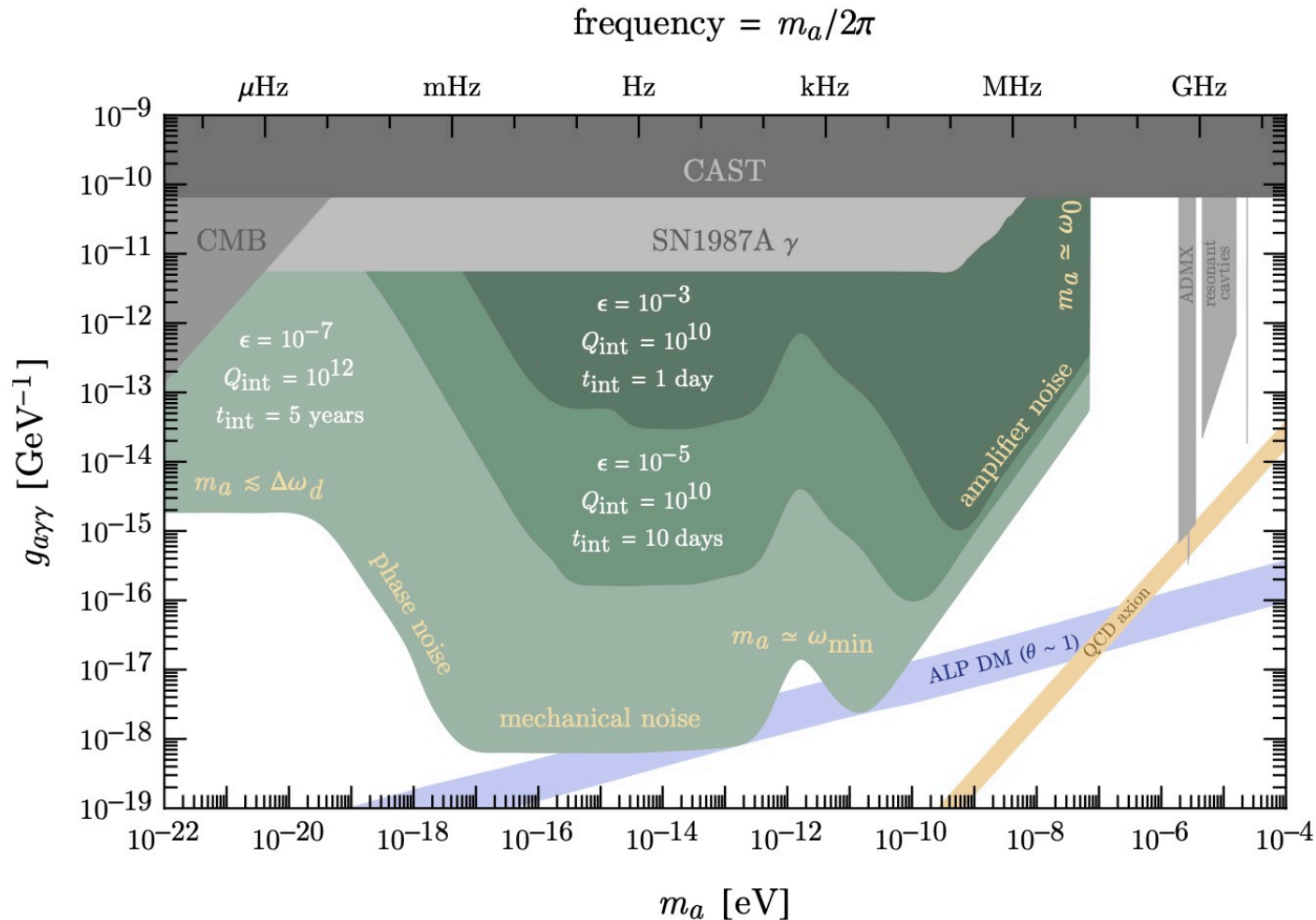
For thermal and readout noise dominant region:

$$\text{SNR} \sim \frac{\rho_{\text{DM}} V}{m_a \omega_1} (g_{a\gamma\gamma} \eta_{10} B_0)^2 \left(\frac{Q_a Q_{\text{int}} t_e}{T} \right)^{1/2}$$

Broadband case

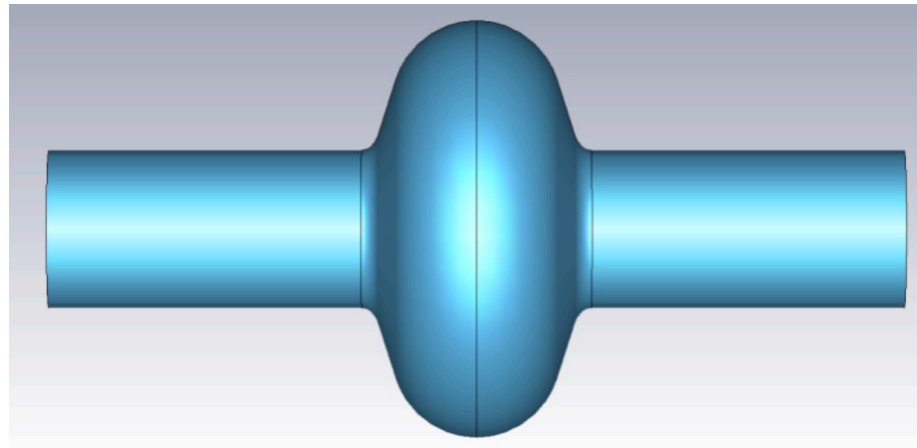
For ultra-light axion, $\omega_1 = \omega_0 + m_a \simeq \omega_0$

Two degenerate and transverse modes can reach the ultra-light region!



Experimental setup

- Collaboration with SRF group, Institute of Heavy Ion Physics, Peking University

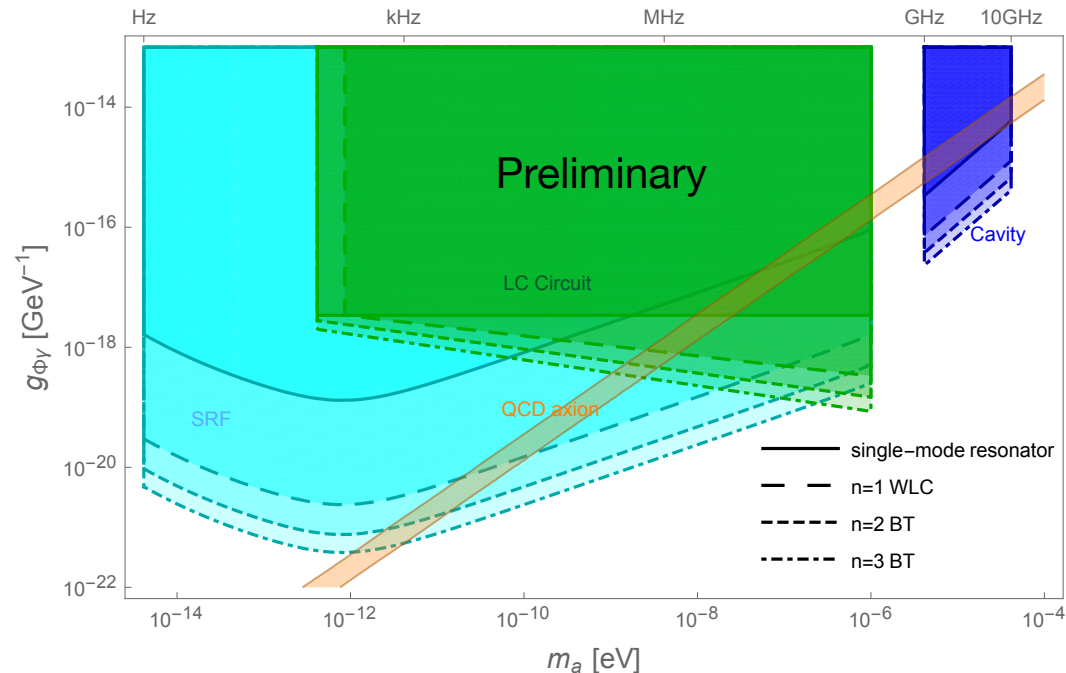


- In progress, quantum limited amplifier designed, cavity noise calibration.
- Path finder with ~ 2 GHz pumping modes and aim for 200 MHz.

Currently the measurements in these region are empty.

Resonator chain and binary tree haloscope

- For single-mode resonator mentioned above, the SNR is bounded by a quantum limit from the readout noise.
- To go beyond quantum limit, one can consider a network of the resonator modes.



- Cover most of the QCD axion dark matter phase space potentially

Conclusion

- The SRF haloscope, with a high quality factor Q and AC magnetic field background, can scan most of the axion dark matter mass window by using both resonant and broadband detection.
- Quantum metrology can play huge roles in the particle physics!

A decorative graphic on a blue background. It features a central white rounded rectangle containing the word "Backup" in red. To the left of the rectangle is a large orange circle, and below it is a smaller green circle. To the right of the rectangle is a green circle above a larger blue circle. A white outline of a circle is positioned above the orange circle. All shapes are connected by thin white lines.

Backup

Low scale Phase Transition



NanoGrav see the “linear power” law for SGWB?

Can it be also be the signal for PT? and how about observations from PPTA?

TOA残差

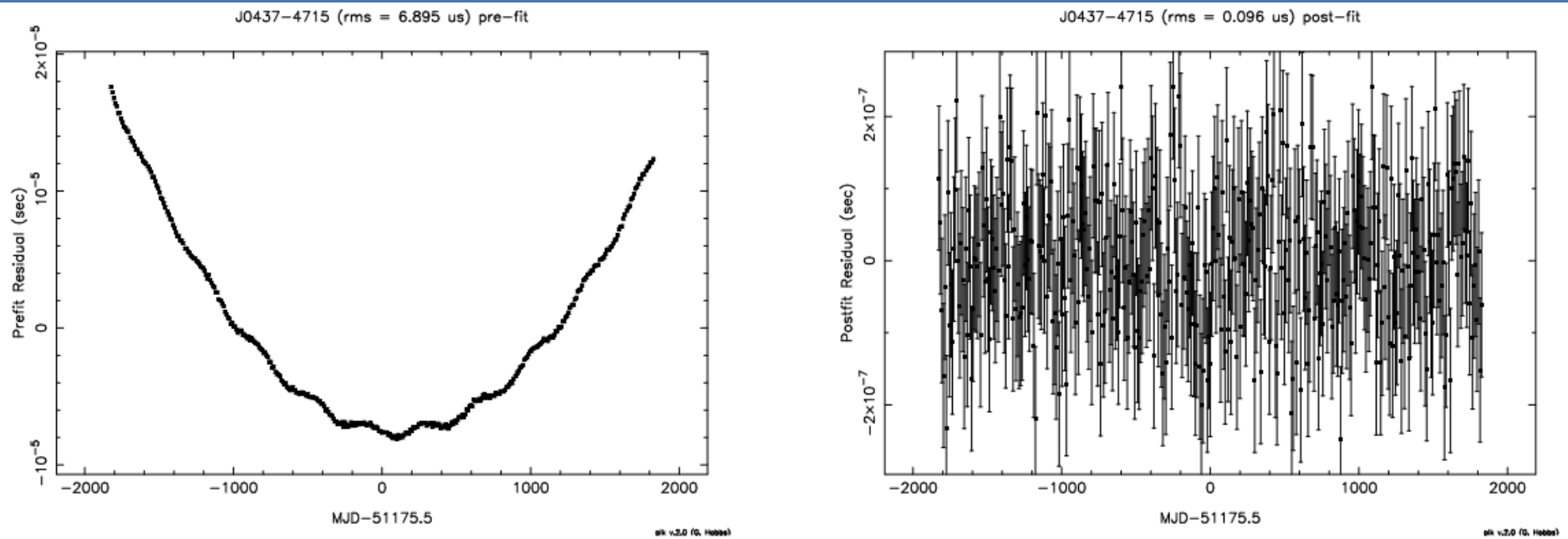
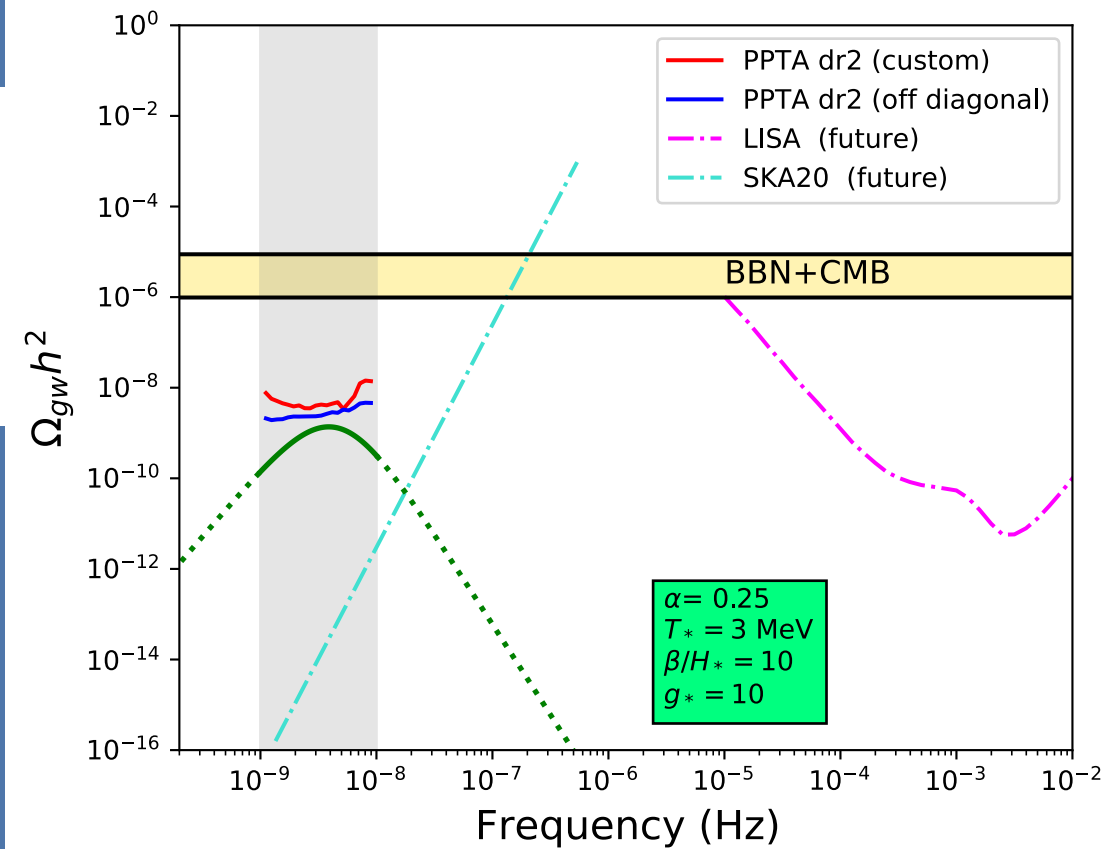


Figure 1: a) pre-fit timing residuals for the test data-set and b) post-fit timing residuals.



浅差

95% Bayesian Exclusion Contour

